THE INFLUENCE OF BRAZING ON VERY COMPACT HEAT EXCHANGER SURFACES

Technical Report No. 73

Prepared under Contract Nonr 225(91)
(NR-090-342)

for

Office of Naval Research

Department of Mechanical Engineering
Stanford University
Stanford, California

November 1, 1970

Report Prepared By:

R. K. Shah
A. L. London

Approved By:

A. L. London
Project Supervisor

ACKNOWLEDGEMENT

The results reported here present a cooperative effort of the Stanford University, Office of Naval Research supported, heat transfer research program and the AiResearch Manufacturing Company, a Division of the Garrett Corporation.

ABSTRACT

Three geometrically similar offset rectangular plate-fin surfaces with area densities in the range from 900 to 2000 ft^2/ft^3 were tested to establish the heat transfer, $j\text{-}N_{R,}$ and flow friction, $f\text{-}N_{R,}$ characteristics. The Reynolds number range was from 60 to 3000. One surface was unbrazed while the other two, because of a two-to-one difference in plate, fin and offset spacing dimensions, were characterized by different degrees of brazing "roughness".

The test results reveal a relatively small effect of brazing on $j\text{-}N_{R,}$ but a significant influence on $f\text{-}N_{R,}$ with a 35 to 50 percent higher friction for the brazed surface. There is an "area penalty" of 14 percent due to brazing associated with the complete coverage of the interface area at the brazed joints. The magnitude of this penalty depends on the geometry of the surface.

TABLE OF CONTENTS

LIST OF TABLES

LIST OF FIGURES

REFERENCES

1. London, A. L., "Laminar Flow Gas Turbine Regenerators -- the Influence of Manufacturing Tolerances," Trans. ASME, J. Engineering for Power, Vol. 92, Series A, 1970, pp. 46-56; also, TR No. 69, Department of Mechanical Engineering, Stanford University, Stanford, California, August 1968.

2. Kays, W. M., and London A. L., "Compact Heat Exchangers," second edition, McGraw-Hill Book Co., Inc., New York, 1964, pp. 138-139.

3. London, A. L., and Shah, R. K., "Offset Rectangular Plate-Fin Surfaces -- Heat Transfer and Flow Friction Characteristics," Trans. ASME, J. Engineering for Power, Vol. 90, Series A, July 1968, pp. 218-228; Condensed from TR No. 66, Department of Mechanical Engineering, Stanford University, Stanford, California, September 1967.

4. Kays, W. M., and London A. L., "Heat Transfer and Flow Friction Characteristics of Some Compact Heat Exchanger Surfaces, Part I - Test System and Procedure," Trans. ASME, Vol. 72, 1950, pp. 1075-1085; also, "Descriptions of Test Equipment and Method of Analysis of Data for Basic Heat Transfer and Flow Friction Tests of High Rating Heat Exchanger Surfaces," TR No. 2, Department of Mechanical Engineering, Stanford University, Stanford California, October 1948.

5. Pucci, P. F., Howard, C. P., and Piersall, C. H.,Jr., "The Single-Blow Transient Testing Technique for Compact Heat Exchanger Surfaces," Trans. ASME, Vol. 89, Series A, Jan. 1967, pp. 29-40.

6. Shah, R. K., "Data Reduction Procedures for the Determination of Connective Surface Heat Transfer and Flow Friction Characteristics -- Steam-to-Air Test Cores," TR No. 64, Department of Mechanical Engineering, Stanford University, Stanford, California, June 1967.

7. Wheeler, A. J., "Single-Blow Transient Testing of Matrix-Type Heat Exchanger Surfaces at Low Values of N_{tu}," TR No. 68, Department of Mechanical Engineering, Stanford University, Stanford, California, May 1968.

8. Klopfer, G. H., "The Design of Periodic-Flow Heat Exchangers for Gas Turbine Engines," TR No. HE-1, Department of Mechanical Engineering, Stanford University, Stanford, California, August 1969.

9. Wiginton, C. L., and Dalton, C., "Incompressible Laminar Flow in the Entrance Region of a Rectangular Duct," Journal of Applied Mechanics, Vol. 37, Trans. ASME, Vol. 92, Series E, 1970, pp. 854-856.

10. Montgomery, S. R., and Wibulswas, P., "Laminar Flow Heat Transfer for Simultaneously Developing Velocity and Temperature Profiles in Ducts of Rectangular Cross-Section," Applied Scientific Research, Vol. 18, 1967, pp. 247-259, Fig. 2 specifically.

11. Sparrow, E. M., Hixon, C. W., and Shavit, G., "Experiments on Laminar Flow Development in Rectangular Ducts," Journal of Basic Engineering, Trans. ASME, Vol. 89, Series D, 1967, pp. 116-124.

12. Young, M. B. O., "Glass Ceramic Triangular and Hexagonal Passage Surfaces -- Heat Transfer and Flow Friction Characteristics," TR No. HE-2, Department of Mechanical Engineering, Stanford University, Stanford, California 1969.

13. London, A. L., Young, M. B. O., and Stang, J. H., "Glass-Ceramic Surfaces, Straight Triangular Passages - Heat Transfer and Flow Friction characteristics," Journal of Engineering for Power, Trans. ASME Vol. 92; Condensed from TR No. 70, Department of Mechanical Engineering, Stanford University, Stanford, California, September 1968.

14. Hall, W. B., Jackson, J. D., and Price, P. H., "Note on Forced Connection in a Pipe Having a Heat Flux Which Varies Exponentially Along its Length," J. Mechanical Engineering Science, Vol. 5, 1963, pp. 48-52.

NOMENCLATURE

English Letter Symbols

a	Plate thickness, in., ft.
A	Total heat transfer surface area, ft^2
A_c	Free flow area on one side of the heat exchanger core, ft^2
A_f	Fin or extended surface heat transfer area, ft^2
A_{fr}	Frontal area of one side, ft^2
b	Plate spacing, distance between plates, in., ft
c	Fin pitch, in., ft
D_h	Hydraulic diameter, $D_h = 4r_h$, ft
d	Plate center to center spacing, $d = b + a$, in.,ft
f	See non-dimensional grouping below
G	Gas mass flow velocity through the core based on A_c, lbm/hr ft^2
g_c	Proportionality factor in Newton's Second Law, $g_c = 32.174$ lbm ft/lbf sec^2
h	Air or gas-side convection heat transfer conductance, Btu/(hr ft^2 °F)
K_c, K_e	Entrance and exit flow loss coefficients, defined in [2], dimensionless
k	Thermal conductivity of the fluid, Btu/(hr ft^2 °F/ft)
L	Test core length in flow direction (plate length), in.,ft
ℓ	Fin length or offset spacing length, in., ft
M	Test core mass, lbm
n	Number of cells in a flow cross section
n_{fin}	Number of fin centers in the test core
n_{off}	Number of offsets in the flow length, see Table V
n_{plate}	Number of plates in the test core
P	Pressure, lbf/ft^2
P	Wetted perimeter of the cell, in., ft

p	Porosity of the core, dimensionless
r_h	Hydraulic radius, defined by $A_c L/A$, ft
t	Temperature, °F
t_{fl}	Fluid temperature just after the step change, °F
V	Flow velocity or total heat exchange volume, ft^3
W	Width of the test core in the direction normal to the stacking of plates and fins, in., ft
w	Air flow rate, lbm/hr

Greek Letter Symbols

α	Ratio of total heat transfer area of one side of the heat exchanger to total exchanger volume, ft^2/ft^3
β	Heat transfer area density, ratio of total heat transfer area on one side of a plate-fin heat exchanger to the volume between the plates on that side, ft^2/ft^3
δ	Fin material thickness, in., ft
η_o	Overall surface temperature effectiveness, dimensionless
μ	Fluid dynamic viscosity coefficient, lbm/hr ft
ρ	Fluid density, lbm/ft^3
τ	An equivalent surface shear stress due to flow friction, including form drag as well as skin friction, lbf/ft^2
τ^*	Dimensionless time, $\tau^* = \frac{hA}{Mc_s}\left(\theta - \frac{wL}{M_f x}\right)$

Nondimensional Grouping

f	Fanning friction factor, $\tau/(\rho V^2/2g_c)$
j	Colburn heat transfer modulus, $N_{St} N_{Pr}^{2/3}$
K_c, K_e	See above
N_{Nu}	Nusselt number for fully developed laminar flow, hD_h/k
N_{Pr}	Prandtl number, $\mu c_p/k$

N_R	Reynolds number based on hydraulic diameter, $D_h G/\mu$
$N_{R,\ell}$	Reynolds number based on uninterrupted fin flow length, $\ell G/\mu$
N_{St}	Stanton number, $h/G\ c_p$
N_{tu}	Number of heat transfer units, hA/wc_p
t_f^*	Fluid temperature, $(t_f-t_i)/(t_{fl}-t_i)$
t_s^*	Wall temperature, $(t_s-t_i)/(t_{fl}-t_i)$
α^*	Aspect ratio of flow passages, $(b-\delta)/(c-\delta)$
ℓ^*	Dimensionless fin offset length, $\ell/4r_h$
δ^*	Dimensionless fin thickness, $\delta/4r_h$

Suffix

Ⓗ	Constant wall heat flux per unit length of the duct with uniform peripheral surface temperature
Ⓣ	Constant wall temperature
f	Fluid
s	Solid or wall
i	Initial, i.e., at time $\theta = 0$

INTRODUCTION

Heat exchangers employing high area density surfaces are of continually increasing technical importance because of one or more of their potential advantages -- low cost, light weight and low bulk. With higher area densities, however, several problems assume a more important role. These are the influence of fouling; the requirements of closer controls on the flow passage-to-passage dimensional variations and fin leading edge details; and the possibly significant influence of brazing on the details of the flow passage geometry which in turn will influence the heat transfer and flow friction characteristics. In less compact surfaces, because of the larger flow passage dimensions these problems are less demanding.

The influence of fouling is so dependent on the details of heat exchanger service conditions that no definitive simple answers are available. For highly compact surfaces it appears that service applications must involve reasonably clean fluids. The importance of manufacturing tolerances has been considered quantitatively in [1][1]. The importance of aerodynamic cleanliness of the leading edges of interrupted-fin surfaces is discussed in [2]. It is the objective of this report to present some limited information relating to the influence of brazing. An additional objective is to provide some better[2] heat transfer, $j\text{-}N_{R,}$ and flow friction, $f\text{-}N_{R,}$ design data for a highly compact offset rectangular plate-fin surface over a wide range of Reynolds number, 60 to 3000.

---

1. Numbers in the bracket denote the numbered references on pp. vii-viii.
2. The present data for Core 501 should be used in lieu of the information previously presented in [3].

DESCRIPTION OF TEST SURFACES

Three offset rectangular plate-fin surfaces, namely, 107, 501 and 501MOD, have been tested for the heat transfer and flow friction characteristics. These surfaces are of the plate-fin strip-fin variety. The general features of the fin center material are depicted in Fig. 1; Table I provides a comparison of the surface geometrical characteristics.

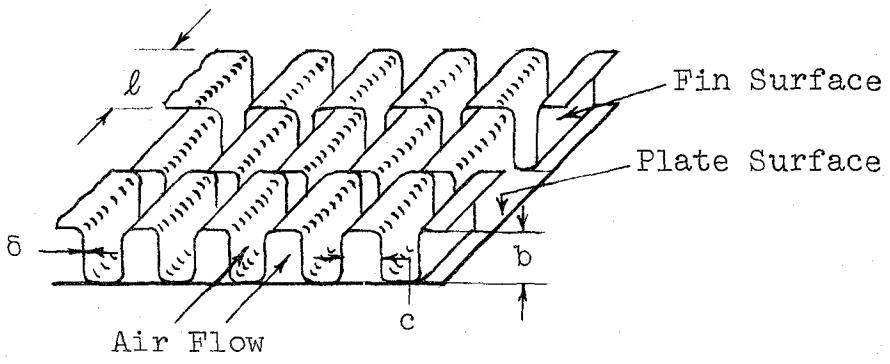

Fig. 1 Fin Center of Offset Rectangular Plate-fin Surface

Surface 107 was built into a core of single sandwich construction for steady state heat transfer testing [4] with a 8-3/8 by 9-3/4 inch test cross section and a 2.03 inch air flow length. The steam side surface was also single sandwich offset rectangular plate-fins with a nominal plate spacing of 1/10 inch, fin offset length of 1/8 inch, and fin pitch of 16 fins per inch. Surface 107 was all stainless steel (AISI 347 type) brazed construction. The fin and plate arrangement for this core is shown in Fig. 2. Test results for this surface are presented previously in [3].

Surfaces 501 and 501MOD were built into cores for the transient heat transfer testing [5] with a 3-1/4 by 3-1/4 inch test cross section and a 2.57 inch air flow length. In Core 501, the fins were separated by plates of 0.006 inch

TABLE I SURFACE GEOMETRY OF OFFSET RECTANGULAR PLATE-FIN SURFACES

(See Figs. 1 and 2)

Core No. (Stanford) AiResearch Designation	107[1]	501[2] PA76451 Eng	501MOD[2] PA 91705
Porosity, $p(= A_c/A_{fr})$		0.744	0.896
Hydraulic diameter, D_h, $(10^{-3}ft)$	4.000	2.118	1.885
Area Density α, ft^2/ft^3		1405	1902
Area Density β, ft^2/ft^3	923	1722	1976
Plate spacing, b, in.	0.0508	0.0265	0.0262
Fin pitch, c, in.	0.0506	0.0271	0.0280
Plate thickness, a, in.	0.006	0.006	0.001
Fin thickness, δ, in.	0.002	0.001	0.001
Fin offset length, ℓ, in.	0.100	0.050	0.050
L/D_h	42.3	101.2	113.2
$\ell^* = \ell/D_h$	2.08	1.97	2.21
Aspect ratio $\alpha^* = (b-\delta)/(c-\delta)$	1.004	0.977	0.933

1. Steady State tests for $j-N_R$
2. Transient tests for $j-N_R$

thickness, and the core was brazed. In Core 501MOD the fins and the plates both were 0.001 inch thick; the fins and the plates were stacked alternatively without brazing. Material for the plates and fins for both cores was stainless steel (AISI 347 type). Test results were reported previously for Core 501 [3]. The present results obtained by improved testing procedures covers a wider N_R range and is recommended in lieu of the previous results. Fig. 2 delineates the fin and plate arrangements for these three cores.

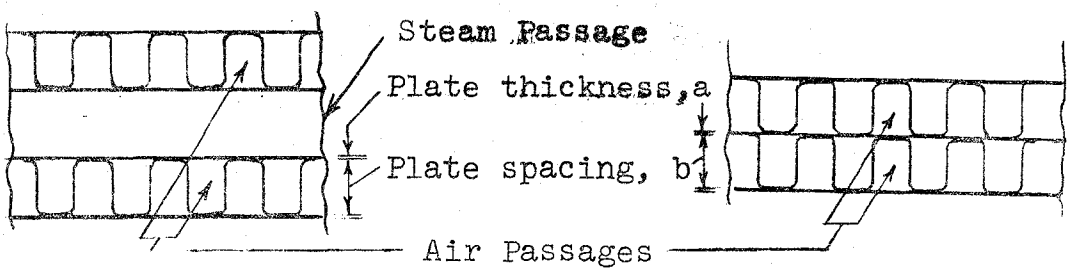

Core 107
(Steady State Tests)

Cores 501 and 501MOD
(Transient Tests)

Fig. 2 Fin and Plate Arrangement of Test Cores

Test core geometries as reported in Table V, Appendix I, were evaluated based on the measurement of fin and plate dimensions and overall test core dimensions. In case of the transient test cores, the porosity was evaluated based on the measured mass and total volume of the test cores. Appendix II outlines the methods used to evaluate the geometrical properties for Core 501 and 501MOD.

EXPERIMENTAL METHODS AND TEST RESULTS

Experimental Methods and Data Reduction Procedures

Core 107 was heat transfer tested by the steady state steam-to-air test technique. The test apparatus and experimental methods are described in [4]. The data reduction procedures are outlined in [6].

Core 501 and 501MOD were heat transfer tested by the transient test technique [5]. The test apparatus, experimental method, and data reduction procedures are described in [7].

All three cores were flow tested by the conventional steady-flow pressure drop measurement. Details of the experimental method and data reduction are provided in both [4] and [6].

Description of Tables and Graphs

The dimensionless heat transfer and flow friction characteristics (the j and f versus N_R plot) of the three cores tested are presented in Figs. 3, 4 and 5. The reduced data from the experimental measurement are given in [3] for Core 107, and in Appendix I for Cores 501 and 501MOD. The test results for Core 501 reported in Appendix I supersedes those in [3], as some measurement errors were found in the air flow rate and the temperature recording equipment. The test results for Core 501MOD reported in Appendix I differs slightly from those in [8] as the fin edge area was not included in the area calculations in [8].

For Core 107, the best interpretation of the friction factor results is faired through the isothermal flow test points. In contrast, the best interpretation of the heat transfer data lie somewhat above the test points due to an allowance for the estimated steam side resistance [3]. For Cores 501 and 501MOD, the best interpretation curves are

both faired through the test points. The coordinates of the best interpretation curves are summarized in Table VII.

Figs. 6 through 10 provide comparisons of the test results for the three cores. Fig. 6 is a comparison based on the hydraulic diameter Reynolds number N_R while the Fig. 7 comparison uses a fin flow length Reynolds number $N_{R,\ell}$. Fig. 8 represents the correlation of test data for the rectangular offset plate-fin surface characterized by $\alpha^* = 1$, $\ell^* = 2$, $\delta^* = 0.04$ based on the experimental results of Cores 501MOD and 107. The flow area goodness factor (the j/f versus N_R characteristics) comparison is made in Fig. 9. The volume area goodness factor (the h_{std} versus E_{std} characteristics) comparison is presented in Fig. 10. These comparisons are discussed later.

For the comparisons made in Fig. 10, the geometries are adjusted to a common hydraulic diameter of 0.002 ft, and the air properties are evaluated at "standard conditions" of dry air at 500 deg F and one atmospheric pressure. The heat transfer power and flow friction power [2,3] for the surfaces are calculated from the following equations.

$$h_{std} = 10.7928\ j\ N_R \quad \text{Btu/(hr ft}^2\ ^\circ\text{F)} \qquad (1)$$

$$E_{std} = 13.6228\ f\ (N_R/1000)^3 \quad \text{hp/ft}^2 \qquad (2)$$

In this way the influence of only the differences in nondimensional geometric factors are revealed, as is already done in Fig. 9 for the flow area goodness factor where the parameters are nondimensional.

Experimental Uncertainty

The evaluation of experimental uncertainty is considered in [4,5,7]. Estimates follow:

Steam-to-air Testing	Transient Testing
$j \pm 5\%$	$j \pm 13\%$
$f \pm 5\%$	$f \pm 3\%$
$N_R \pm 2\%$	$N_R \pm 2\%$

The repeatability of the test points by different experimeters, at different times, but using the same transient test rig [7] is within five percent for j and two percent for f factors. The scatter of the j points on Figs. 4 and 5 is less than five percent. These factors suggest that the uncertainty predictions for the j factors of $\pm$ 13 percent for the transient testing may be conservatively too high.

The following factors are not considered in the uncertainty analysis:

1. Malflow distribution through the core due to partial passage blockage arising from poor brazing or from bent fin offset edges.
2. Surface roughness due to the braze coating and form drag from brazing beads fused to the surface.

Fig. 3 PLATE-FIN SURFACE HEAT TRANSFER AND FRICTION CHARACTERISTICS
Core 107. Surface 19.74R(S) - .0510/.0508 - 1/10(0) - .002(SS)

Surface Data - Air Side:

Fins per inch = 19.74

Plate spacing, b = 0.0508 inch

Fin offset length (flow direction), ℓ = 1/10 inch

Flow passage hydraulic diameter, $4r_h$ = 0.004000 ft

Fin metal thickness = 0.002 inch

Total heat transfer area/volume between plates

β = 922.8 ft^2/ft^3

Fin area/total area = 0.923

O - Hot core test points. Heat transfer data evaluated on the basis of zero steam-side resistance

X - Cold core friction factors

Best interpretation of friction data based on cold core data.

Best interpretation of heat transfer data based on an allowance for steam side resistance.

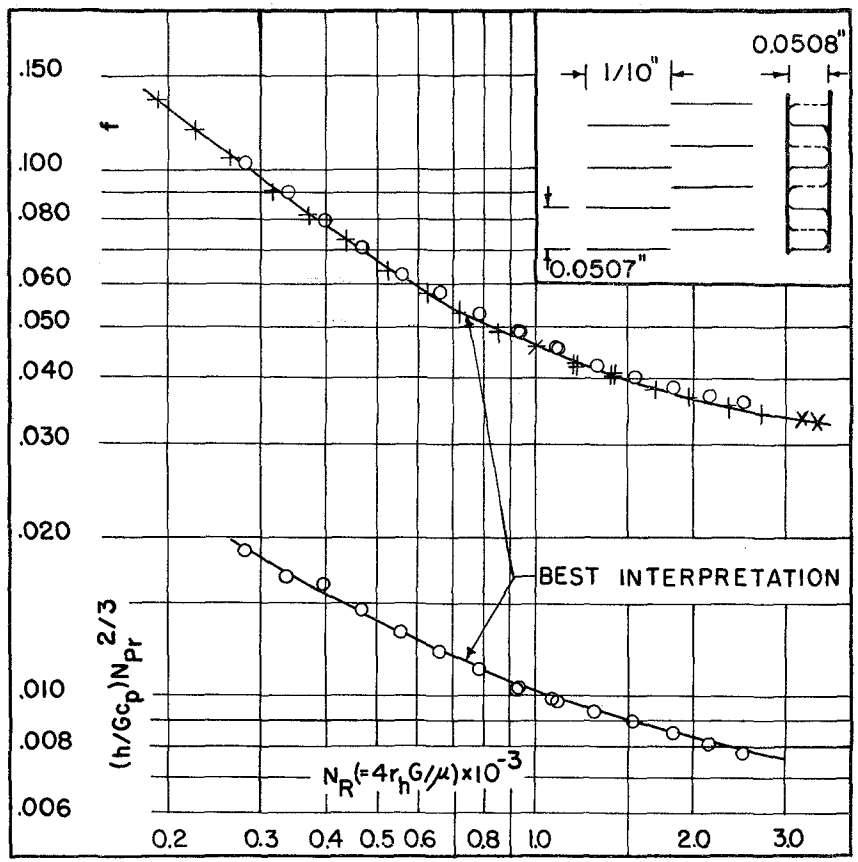

Fig. 4 PLATE-FIN SURFACE HEAT TRANSFER AND FRICTION CHARACTERISTICS
Core 501. Surface 36.85R - .0265/.0265 - 1/20(0) - .001(SS)

Surface Data:

Fins per inch = 36.85
Plate spacing = 0.0265 inch
Fin length (flow direction), ℓ = 1/20 inch
Fin metal thickness = 0.001 inch
Plate metal thickness = 0.006 inch bare
0.008 inch under fins (braze build up)
Flow passage hydraulic diameter, $4r_h$ = 0.002118 ft
Total heat transfer area/volume between plates, β = 1722 ft^2/ft^3
Total heat transfer area/total volume, α = 1405 ft^2/ft^3
Porosity, p = 0.744

□ - Transient test technique data points for heat transfer

0 - Cold core (steady state) data points for friction factors

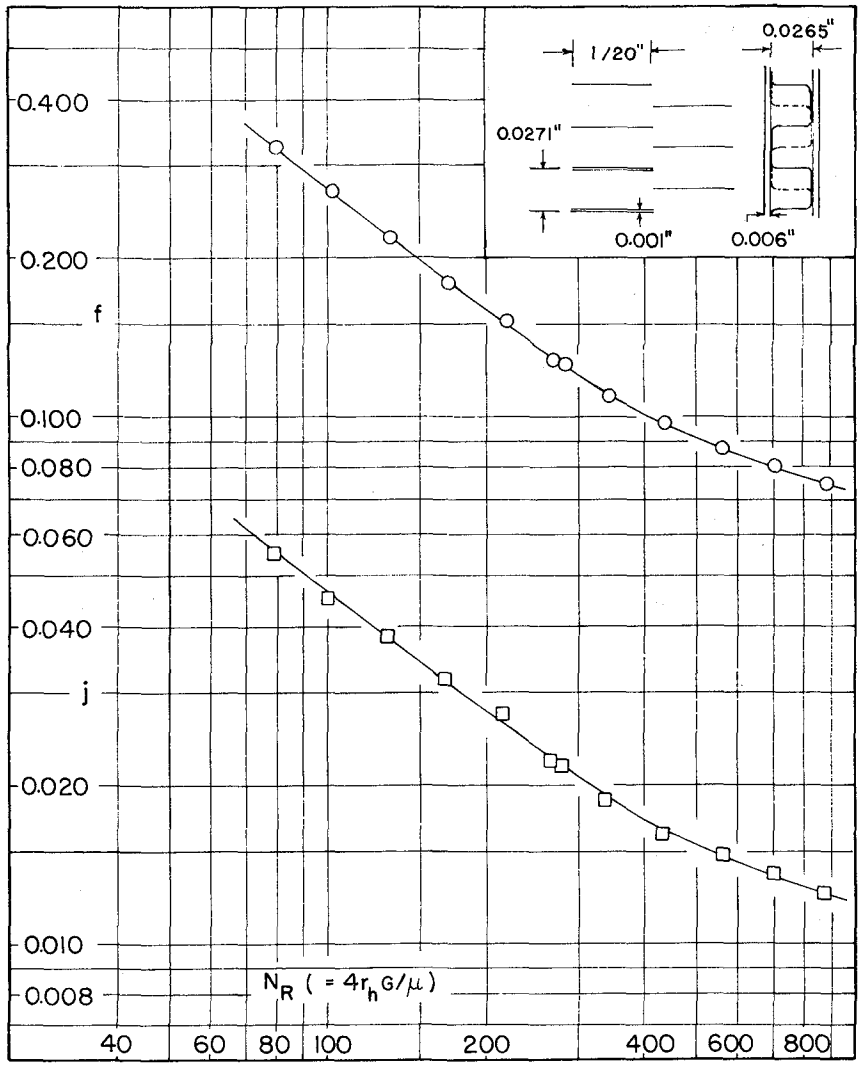

Fig. 5 PLATE-FIN SURFACE HEAT TRANSFER AND FRICTION CHARACTERISTICS
Core 501MOD Surface 35.74R(S) - .0262/.0262 - 1/20(O) - .001(SS)

Surface Data:

Fins per inch = 35.74
Plate spacing, b = 0.0262 inch
Fin length (flow direction) ℓ = 1/20 inch
Fin metal thickness = 0.001 inch
Plate metal thickness = 0.001 inch

Flow passage hydraulic diameter, $4r_h$ = 0.001885 ft
Total heat transfer area/volume between plates
β = 1976 ft^2/ft^3
Total heat transfer area/total volume
α = 1902 ft^2/ft^3
Porosity p = 0.896

□ - Transient test technique data points for heat transfer
O - Cold Core (steady state) data points for friction factors

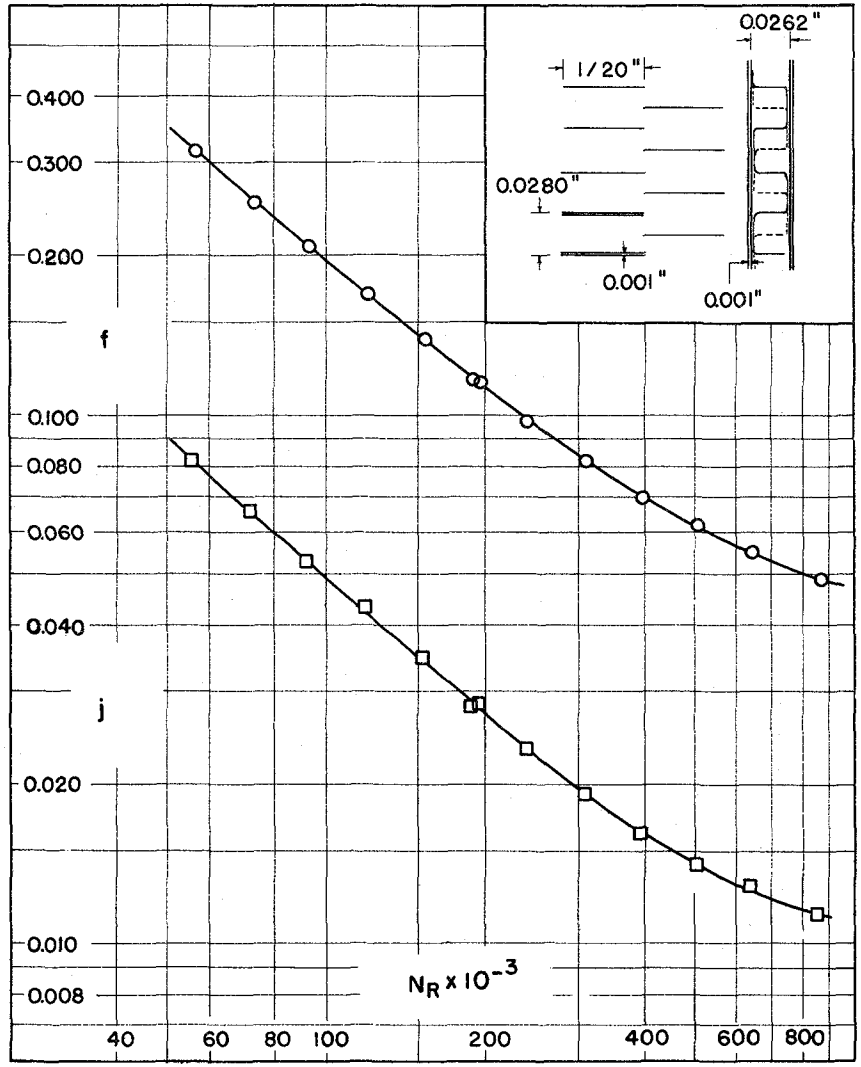

DISCUSSION

All three test cores, aside from the influence of brazing, have surfaces that are closely similar geometrically, as can be seen by comparisons provided in Table II.

TABLE II Nondimensional Geometry Comparison

Core	δ^*	ℓ^*	α^*	A_f/A	βr_h
107	0.042	2.08	1.00	0.508	0.923
501	0.039	1.97	0.98	0.481	0.913
501MOD	0.044	2.21	0.93	-	0.931

However, the Core 107 surface has about twice the scale of the other two, as can be seen from the hydraulic diameter ($4r_h$) line in Table III, where other differences in construction and testing techniques are summarized.

TABLE III Core Construction and Testing Differences

Core No.	501	501MOD	107
Hydraulic Diameter $4r_h$ (10^{-3}ft)	2.118	1.885	4.000
Brazed Construction	yes	no	yes
Testing Technique:			
j - N_R	trans.[1]	trans.	steam heat (ss)
f - N_R	(ss)[2]	(ss)	(ss)

[1]Transient single blow technique
[2]Steady State technique (ss)

Because of the two-to-one dimension ratio of the Core 107 surface relative to the 501 surface, the realtive roughness due to brazing should be in the ratio of one-to-two. The 501MOD surface in contrast should be representative of a smooth surface.

While the f-N_R characteristics for the three surfaces, Fig. 6, were all established using the common fluid flow steady-state technique, the heat transfer testing employed a steady state steam heating technique for Core 107 while the single blow transient technique was used for the other two cores. It appears that these different test techniques yield about the same j-N_R characteristics, Fig. 6, corresponding to approximately the constant wall temperature boundary condition of the Core 107 tests. A discussion of this aspect is presented in Appendix III.

A final important difference that is not shown in Table III is the fact that different geometrical models were used to evaluate the β (or α) and r_h dimensions for the three surfaces. These models are shown in Fig. 11. Originally, the ideal rectangular model (Fig. 11a,c) was used for all three cores, but after high magnification visual inspection it was concluded that the unbrazed surface did not have as complete mechanical contact between the fins and plate, and consequently,more area was available for heat transfer. Fig.11b was then proposed for the 501MOD core surface. Appendix II presents the detailed considerations leading to the geometrical parameters of Table I. It also contains the equations for porosity, area density and hydraulic radius leading to the following comparison, Table IV.

TABLE IV Core 501MOD Geometries Derived From Different Models

	Table I	Rectangular Model Fig. 11c	Modified Model Fig. 11b
Cell dimensions (inches)			
cell height, d	0.0272		
cell width, c	0.0280	same	same
fin thickness, a	0.001		
plate thickness, δ	0.001		
Area density, α ft^2/ft^3	1902	1640	1902
Porosity, p	0.896[1]	0.893	0.902[2]
Hydraulic radius, r_h (10^{-4} ft)	4.71	5.47	4.71

1. Porosity determined gravimetrically, see Appendix II.
2. The agreement with the Table I porosity magnitude demonstrates that the plate and fin thicknesses are indeed close to the nominal magnitude of 0.001 inches.

From this comparison it is evident that the two models, Fig. 11b and c, lead to virtually the same result for the porosity, but that the unbrazed model, Fig. 11b, yields the higher area density (and lower r_h as a consequence) by about 14 percent. This area difference might be considered as an area coverage penalty paid for brazing due to geometrical considerations. Inspection of Fig. 11 leads to the conclusion that this penalty decreases as the ratio of fin area to plate area increases. For these surfaces, because of the close to square flow cross-section ($\alpha^* \approx 1$), the fin-to-plate area ratio is about one. For deep-fold surface [1], the area coverage penalty is substantially smaller. Clearly, in direct transfer heat exchangers where brazing is needed to insure adequate fin heat transfer performance the term "area coverage penalty" is a misnomer. However, for the periodic-flow type exchanger where brazing may be used only for structural

stability the resulting surface coverage does indeed result in an area penalty from a heat transfer point of view.

As can be seen from Fig. 6, the three surfaces do indeed exhibit quite closely the same j-N_R characteristics as expected from their close geometrical similarity. A $\pm$ 10 percent band about the mean would include all three characteristics. As discussed in [3], the gross blockage due to brazing would reduce the j slightly. From the comparison of Fig. 6 this can be seen at low Reynolds numbers. The different slope of the j-N_R curves may be partially due to a 10 percent difference in ℓ^* shown in Table II. Possibly brazing roughness does tend to produce an earlier transition to a turbulent flow behavior, as evidenced by the j-N_R tendencies for the two brazed cores at the higher Reynolds numbers. A conclusion then, is that aside from the influence of brazing in reducing the heat transfer surface area, there is no major influence of brazing roughness on the j-N_R behavior.

Core 501, having thicker plates than the fins and having good thermal contact due to brazing, may exhibit "fin effect" for the transient test conditions. This behavior does not apply to Core 501MOD as the plates and fins are of the same thickness and have poor thermal contact. Calculations for the steady-state heat transfer show that the overall fin effectiveness η_o for the Core 501 geometry varies from 0.995 to 0.975 for the variation in h from 10 to 75 Btu/hr ft^2°F. As the transient η_o is always higher than that for the steady state condition, it was concluded that there was no significant "fin effect" $(1-\eta_o)$ on the Core 501 data.

In contrast to the small influence of brazing on the j-N_R characteristics, the f-N_R characteristics is strongly influenced. The surface with the greater relative roughness (Core 501) has 35-50 percent higher friction factor relative to the smooth surface (501MOD). The 107 surface with its

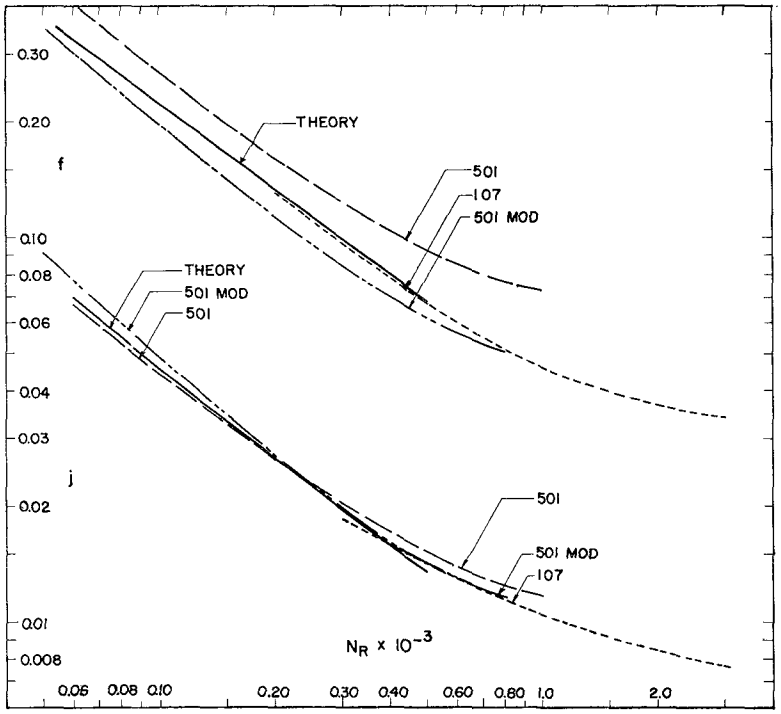

Fig. 6 Hydraulic Diameter Reynolds Number Comparisons for Surfaces 107, 501, 501MOD

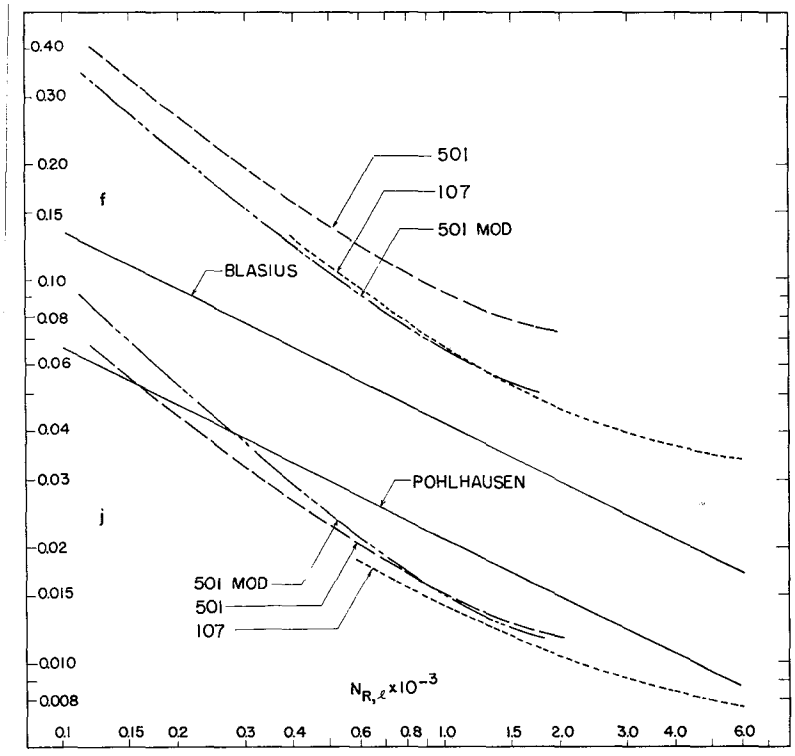

Fig. 7 Offset Spacing Reynolds Number Comparisons for Surfaces 107, 501, 501MOD

intermediate roughness has an intermediate behavior. The theory curves of Fig. 6 will be discussed shortly.

The same relative behavior for j-N_R and f-N_R appear in Fig. 7 where an $N_{R,\ell}$ abscissa is used. Also shown are the theory lines for very thin short flat plate behavior, as deduced from the Pohlhausen solution for heat transfer with uniform surface temperature and the Blasius solution for skin friction.

In this comparison it is evident that the skin friction effect, as represented by the Blasius solution, amounts to only half of the flow friction represented by f of the test surfaces. The axial pressure gradient in the developing flow through a duct is higher than that over a flat plate due to the periodic flow accelerations (over each fin offset) and higher wall shear caused by higher transverse velocity gradients. The approximate 100 percent higher f factors for Core 501MOD from the Blasius solution can account for this effect. From hydrodynamic entry length solution,

$$\frac{\Delta P}{1/2\ \rho V^2} = \phi\ \left(\frac{x}{D_h N_R}\right)$$

where ϕ stands for the functional relationship. For each fin offset the pressure drop is evaluated at $x = \ell$. The larger the $\ell/D_h N_R$, the higher the pressure gradient. As a result, the departure from Blasius solution is increased at lower Reynolds number. The incrementally higher friction factor for Core 501, however, cannot be attributed to the above mentioned effects as the fin passages are not significantly different from those of Core 501MOD. Visual inspection of the 501 Core did indeed reveal some bridging of the offset fin edges by "uncommitted" brazing material.

Comparison with Pohlhausen solution indicates lower heat transfer behavior for the surfaces tested. The simplified theory line of Fig. 7 assume that all the surface has interruptions which is contrary to fact as only the vertical fin surfaces of Fig. 1 are interrupted, about 50 percent of the total, while the plate surface, combined with the horizontal center material surface, may be described as a somewhat roughened uninterrupted surface. The average heat transfer coefficient over the uninterrupted surface is lower than the interrupted surface with the result that the heat transfer coefficient for the test surfaces should be lower than the Pohlhausen solution.

In this vein, a theory model was devised as follows consisting of 50 percent of the surface square section tubes with $\ell/D_h = \infty$, and 50 percent of the surface square section tubes with $\ell/D_h = 2$. Then

$$f_{Model} = 0.5\, f_{\ell/D_h=2} + 0.5\, f_{\ell/D_h=\infty} = 0.5(f^* + 1) f_{\ell/D_h=\infty} \qquad (3)$$

$$j_{Model} = 0.5\, j_{\ell/D_h=2} + 0.5\, j_{\ell/D_h=\infty} = 0.5(j^* + 1) j_{\ell/D_h=\infty} \qquad (4)$$

where f^* and j^* are the normalized values for the short tubes relative to the long tubes.

The required f and j information is available for $\ell/D_h = \infty$, that is fully developed flow in square section tubes, in [2].

$$f_{\ell/D_h = \infty} = \frac{14.227}{N_R}$$

$$j_{\ell/D_h = \infty} = \frac{3.35}{N_R} \text{ (for } N_{Pr} = 0.7,\ N_{Nu,\textcircled{T}} = 2.976)$$

For the short square tube, the hydrodynamic entry length solution of Wiginton and Dalton [9][1] is used to evaluate f^*. While the combined hydrodynamic and thermal entry length solution of Montgomery and Wibulswas [10] is employed to determine j^*. The (T) boundary condition is used, as each short interrupted fin is essentially at a uniform surface temperature at any instant of time.

This was the technique used to provide the theory curves shown in Figs. 6 and 8. It is evident that this theory model does indeed provide a very good prediction of performance for heat transfer; but the friction factor prediction is somewhat higher than the smooth Core 501MOD behavior, ranging from 16 percent at $N_R = 200$ to 6 percent at $N_R = 500$.

From Fig. 6, the higher f factors (0-17 percent) for Core 107 in comparison to Core 501MOD can partially be accounted for by the small differences in ℓ^* (2.08 versus 2.21, Table II), and partially due to brazing surface roughness. The difference of about 35-50 percent in f factors for Cores 501 and 501MOD is too large to attribute to the ℓ^* effect (1.97 versus

[1]The hydrodynamic entry length theory results for the rectangular ducts by Ref. [9] are in excellent agreement with the experimental work of Sparrow et al. [11].

2.21). The difference is quite constant over the N_R range and probably must be charged to brazing surface roughness and brazing material flow blockage. The pressure drop in the core is proportional to $1/p^3$. Hence the influence of brazing on the "free flow area" porosity will have an amplified effect on the pressure drop resulting in higher friction factors. Even if the higher friction of Cores 107 and 501 compared to Core 501MOD is attributed entirely due to brazing influences, there is significantly less effect of brazing for Core 107 in relation to Core 501, as Core 107 has only one half the non-dimensional brazing surface roughness characterization. One may conclude that the influence of brazing on friction is a strong function of the compactness of the surface.

Based on the test results of Cores 501MOD and 107, the $f\text{-}N_R$ and $j\text{-}N_R$ characteristics for geometrically similar smooth surfaces defined by $\alpha^* = 1$, $\ell^* = 2$, $\delta^* = 0.04$ are presented for a Reynolds number range of 60 to 3000 as shown in Fig. 8. On this figure are also drawn the theory line based on the model described previously. The ordinates of Fig. 8 are presented in Table VII. This somewhat generalized result, plus the kind of modeling as represented by the theory characteristics, may be useful to the designer who wishes to make modest extrapolations from the geometry of the test core surfaces. The surface characteristics of the idealized rectangular offset plate-fin surface of Fig. 8 do not take into consideration the gross blockage due to the brazing and the brazing roughness. The brazing has a relatively small effect on the $j\text{-}N_R$, but a significant influence on $f\text{-}N_R$ with increased friction for a more compact surface.

Incidentally, unlike the continuous laminar flow passages, this offset rectangular plate-fin surface is not significantly influenced by random passage-to-passage non-uniformities.

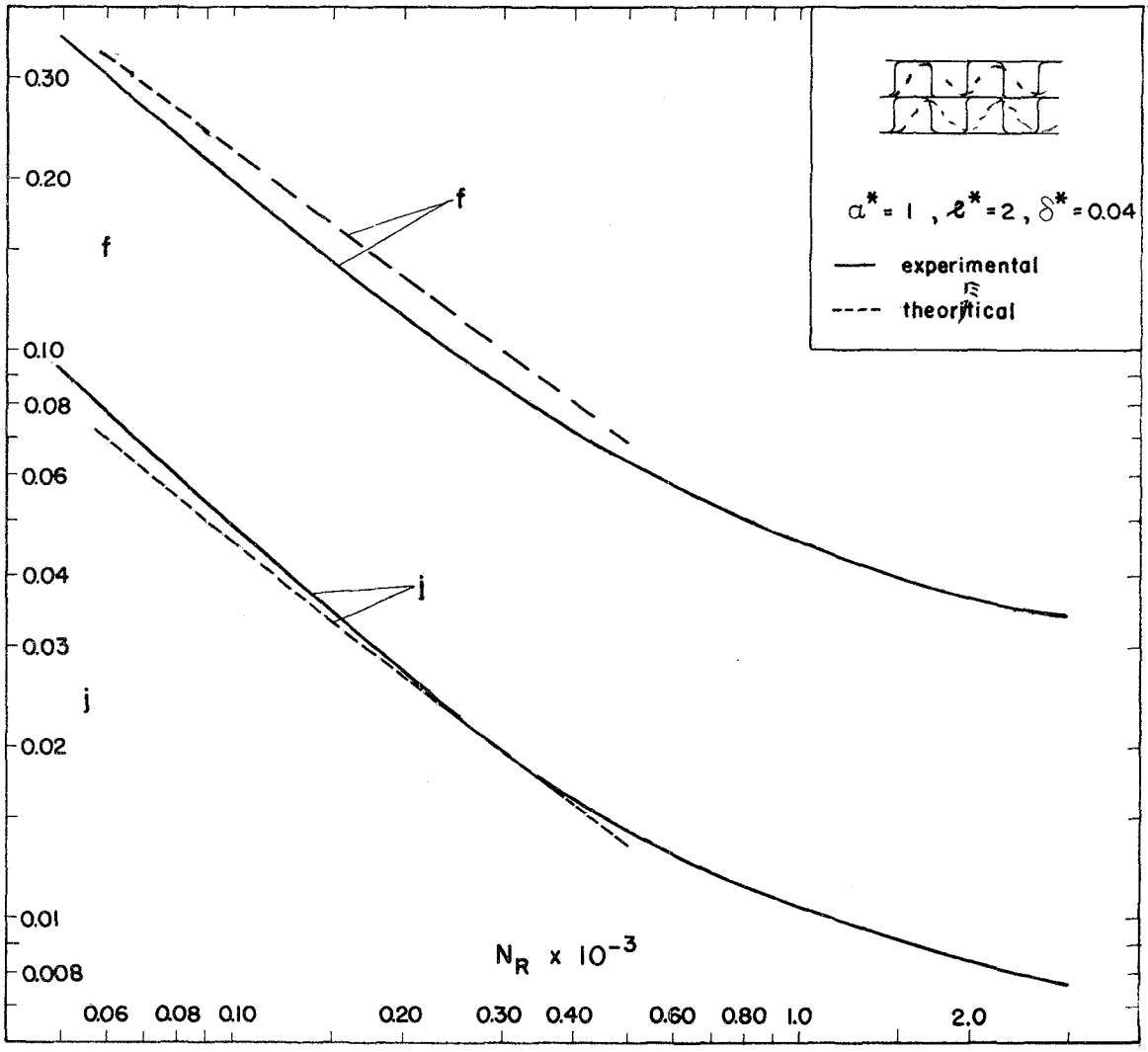

Fig. 8 Correlation of Experimental Data for the Offset Rectangular Plate-Fin Surface having $\alpha^* = 1$, $\ell^* = 2$, $\delta^* = 0.04$

As discussed in Ref. [1], the passage-to-passage non-uniformity can have a substantial effect on the j-N_R characteristics of a continuous surface.

Goodness Factors

The j/f versus N_R plot of Fig. 9 is of interest to the designer as j/f may be considered a flow area goodness factor. It can be shown that

$$\frac{j}{f} = \frac{N_{Pr}^{2/3}}{2g_c\rho} \frac{N_{tu}\, w^2}{\Delta P} \frac{1}{A_c^2} \qquad (5)$$

In a heat exchanger designed for a given performance, the effectiveness ϵ, the fluid thermal capacity rate ratio C_{min}/C_{max}, the pressure drop ΔP, and the fluid flow rate w are specified. The number of heat transfer units, N_{tu}, is fixed for a given ϵ, fluid flow rates, and the flow arrangement. Thus the ratio j/f is inversely proportional to A_c^2, where A_c is the free flow area. A larger j/f makes a smaller free flow area and hence generally the smaller frontal area of a heat exchanger. From Fig. 9, as the j/f ratio for Core 501MOD (and 107) is about 50 percent higher than that for Core 501, there is, as a consequence, a penalty of about 22 percent in the free flow area requirement attributed to brazing. Core porosity must also be considered in order to translate the free flow area penalty into a frontal area penalty.

Note that in the flow area goodness factor comparison, no estimate of total heat transfer area or the volume can be inferred. In contrast, Fig. 10 provides volume goodness factors by a plot of h_{std} versus E_{std}, where

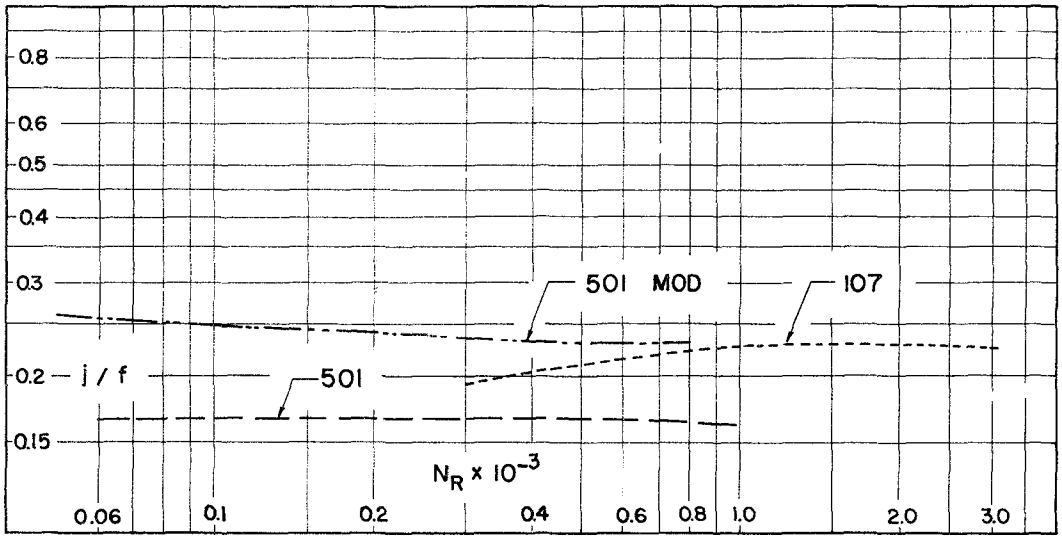

Fig. 9 Flow Area Goodness Factor Comparisons for Surfaces 107, 501, and 501MOD

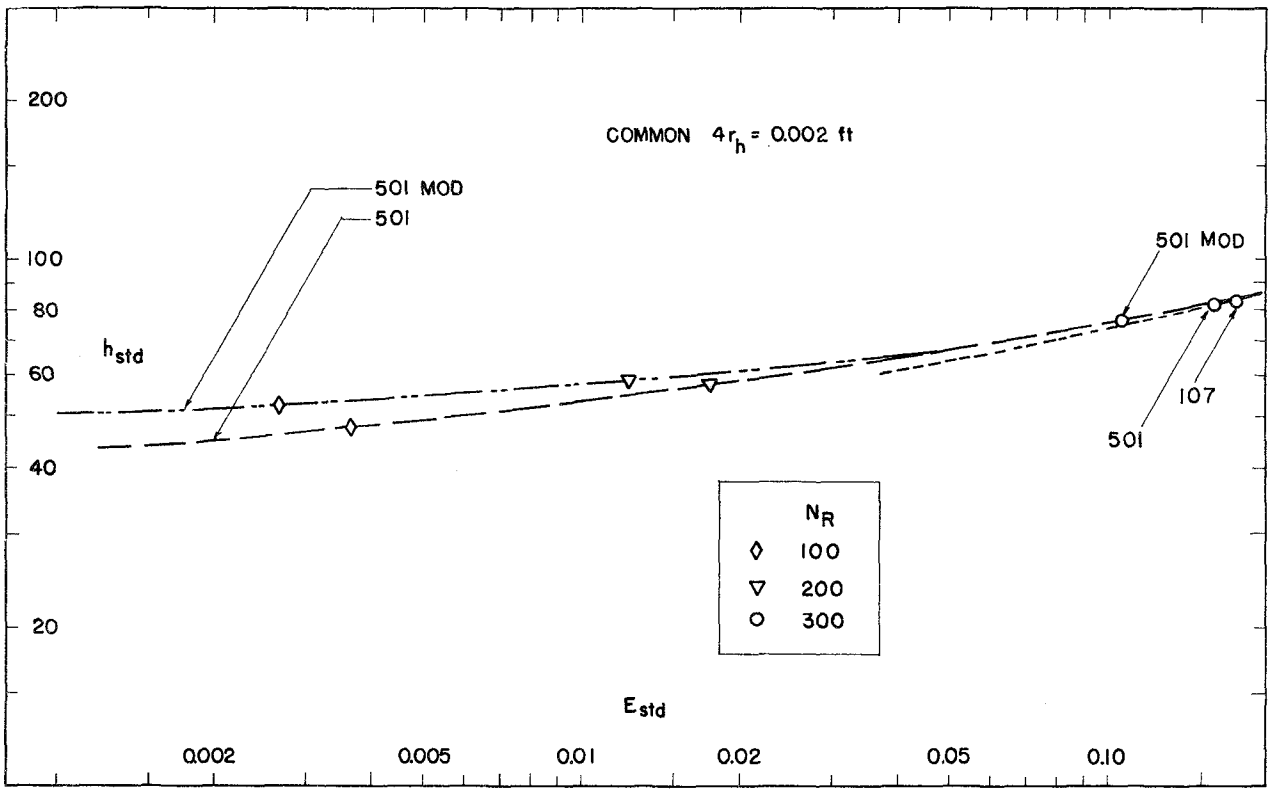

Fig. 10 Volume Goodness Factor Comparison for Surfaces 107, 501, and 501MOD

$$h_{std} = \frac{c_p \mu}{N_{Pr}^{2/3}} \frac{1}{4r_h} jN_R \quad \text{Btu/(hr ft}^2\text{°F)} \tag{6}$$

$$E_{std} = \frac{\mu^3}{2g_c \rho^2} \left(\frac{1}{4r_h}\right)^3 fN_R^3 \quad \text{hp/ft}^2 \tag{7}$$

A common hydraulic diameter $4r_h = 0.002$ ft is used to eliminate the influences of the scale of the surface geometries and thereby gain an insight as to the influence of brazing alone. Air properties at one atmosphere and 500 deg F are used to arrive at the h_{std} and E_{std} in Eqs. (1) and (2).

The higher heat transfer power per unit area and potential difference h_{std}, for a given fluid pumping power (per unit area) E_{std}, the lower is the exchanger heat transfer area A (= αV or βV as appropriate) requirement; since α or β is proportional to $1/r_h$, and r_h is fixed, the smaller is the heat exchanger volume for a given porosity. At a typical E_{std} of 0.005 hp/ft^2 the aerodynamically cleanest surface, Core 501MOD, has about 11 percent (55/49.5) higher heat transfer power in comparison to the Core 501 surface, thus requiring 10 percent (1-1/1.11) less heat transfer area and, at the same time,about 10 percent less pressure drop ($\Delta P \propto A\, E_{std}$). These penalties for Core 501 are due primarily to effect of brazing on flow friction.

SUMMARY AND CONCLUSIONS

The main features of this report are summarized here.

1. The basic heat transfer, $j\text{-}N_R$, and flow-friction $f\text{-}N_R$ characteristics of three close to geometrically similar offset rectangular plate-fin surfaces are presented in Figs. 3, 4 and 5 and in Table VII. Cores 501 and 501MOD have identical fin centers of 0.001 in. thick stock, but different plate thicknesses, 0.006 and 0.001 inches, respectively. Core 501 is brazed while Core 501MOD is unbrazed. The steam Core 107 is also brazed, but has almost double sized fin centers compared to the other two. Core 107 was heat transfer tested using a steady-state steam to air testing technique. In contrast, the other two surfaces were heat transfer tested using a transient technique. All three cores were flow-tested using the conventional steady flow pressure drop technique. The main purpose of these tests was to investigate the influence of brazing on both heat transfer and flow friction.

2. The influence of brazing on heat transfer, the $j\text{-}N_R$ characteristics, is minor. However, brazing does result in coverage of surface at the brazed joints and, as a consequence, there is an area penalty, in the case of the aspects ratio $\alpha^* \approx 1$ geometry of these cores, of approximately 14 percent. For deep-fold surfaces of high aspect ratio [1], this area penalty is much lower.

3. The influence of brazing on flow friction, the $f\text{-}N_R$ characteristics, is quite significant, amounting to 35-50 percent higher for the braze rough 501 core relative to the smooth surface 501MOD Core. Brazing rough-

ness appears to be of two types, a fine grained surface roughness and that produced by the flow of excess braze material during the fusion process, so as to partially block the flow passage by bridging the offset gap on the fins. The influence of brazing roughness decreases as the surface becomes less compact, because then the nondimensional roughness, obtained by normalizing with respect to D_h, is reduced, and also one would expect bridging of the offset gap to be reduced.

4. In a given heat exchanger application, even after discounting the 14 percent area penalty associated with joint coverage, the brazed 501 surface would require a 22 percent greater frontal area and a possible 10 percent greater bulk in relation to the 501MOD surface. This is the magnitude of the brazing penalty for very compact surfaces with area densities of the order of 2000 ft^2/ft^3. For lower area densities the penalty is reduced proportionally.

5. Fig. 8 provides a generalization of the test results, excluding the influence of brazing roughness on $f\text{-}N_R$, that may prove useful for design purpose.

APPENDIX I

TEST CORE GEOMETRICAL DATA, REDUCED LABORATORY DATA AND COORDINATES FOR THE SMOOTHED CURVES OF FRICTION AND HEAT TRANSFER CHARACTERISTICS

In this appendix, the information needed for re-evaluation of any test data is summarized.

Test Core Geometrical Data, Table V

All of the core geometrical data to reduce the direct laboratory data are summarized in Table V. The method employed to evaluate the core properties of the transient test matrices is outlined in Appendix II.

Reduced Laboratory Data, Table VI

The reduced laboratory data for Cores 107 and 501 are presented in Refs. [3] and [8], respectively. The reduced experimental data for Cores 501 and 501MOD are given in Table VI, for the completeness of the report, although the reduced data for Core 501 are available in [8]. The test results for Core 501 reported in [8] supersedes those in [3], as some measurement errors were found in the air flow rate and the temperature recorder. The test results for Core 501MOD reported in Table VI supersede those in [8], as the fin edge area was not included in the heat transfer area calculation and subsequent geometrical properties; also an error was found in the core dimensions of [8]. The fin edge area is about 1 to 1.5% of the total heat transfer area.

The laboratory data were processed on an IBM 360/67 computer based on the data reduction procedure in Ref. [7]. The test results are presented in Table VI, and are plotted in Figs. 5 and 6 (Core 501, 501MOD).

Best Interpretation Surface Characteristics, Table VII

The curves of Figs. 3-5 are drawn so as to represent the best interpretation of the reduced laboratory data in terms of the f and j versus N_R characteristics of the surfaces. For Core 107, the best interpretation of the friction factor results is faired through the isothermal flow test points; while the best interpretation of the heat transfer data lie somewhat above the test points due to an allowance for the estimated steam side resistance [3]. For Cores 501 and 501MOD, the best interpretation curves are drawn smoothly through the actual test points; the physical properties and air flow rate are evaluated based on the arithmetic mean temperature. The coordinates of the best interpretation or smoothed curves are summarized in Table VII.

Table V Actual Test Core Geometrical Data

Core No. (Stanford)	107	501	501MOD
Core Dimensions, inches			
Width	8.641	3.243	3.327
Height	9.606	3.248	3.348
Flow length, L	2.031	2.57	2.562
Uninterrupted fin length, ℓ	0.100	0.050	0.050
Fin pitch, c	0.0506	0.0271	0.0280
Plate spacing, b[1]	0.0508	0.0265	0.0262
Plate thickness, a	0.006	0.006	0.001
Fin thickness, δ	0.001	0.001	0.001
Number of plates, n_{plate}	-	101	124
Number of fin centers, n_{fin}	57	100	123
Number of offsets per fin center, n_{off}	20	50	50
Number of fins per inch	19.74	36.85	35.74
Frontal area A_{fr}, in.^{2}	24.642[1]	10.533	11.139
Free flow area A_c, in.^{2}	22.737	7.838	9.986
Conduction area A_s, in.^{2}	-	2.28	0.721
Core volume V, in.^{3}	-	27.07	28.54
Core mass M, lbm	-	1.956	0.8345
Porosity p	-	0.7441	0.8965
Area density α, ft^2/ft^3	-	1405	1902
Area density β, ft^2/ft^3	923	1722	1976
Hydraulic diameter D_h, (10^{-3}ft)	4.000	2.118	1.885
L/D_h	42.2	101.2	113.2
ℓ/D_h	2.08	1.97	2.21
Solid density ρ_s, lbm/ft^3	-	488	488
Solid specific heat c_s, Btu/lbm °F	-	0.112	0.112
Solid thermal conductivity k_s, Btu/hr ft °F (at mean test temp.)	8.9	8.3	8.3
K_c	0.38	0.19	0.08
K_e	0.53	0.06	0.02

[1]Measured between plates.

Table VI Experimental and Reduced Laboratory Data for Core 501

SINGLE-BLOW TRANSIENT TEST DATA

CORE NO. 501 AIRES. PLATE-FIN DATA TAKEN ON MARCH 28, 1968 DATA TAKEN BY KLOPFER

THE FOLLOWING ARE INPUT TEST DATA

RUN	DPOC	DPOH	P1OC	P1OH	T1OC	T1OH	DPS	P1S	T1SC	T1SH	DTAU	TDB	TWB	PAMB
THE FOLLOWING DATA ARE TAKEN WITH 1.3015 INCH ORIFICE														
1	0.790	0.810	1.210	1.260	0.899	1.212	1.140	0.058	0.888	1.260	28.800	72.0	59.0	409.32
2	1.290	1.310	1.630	1.700	0.911	1.244	1.530	0.082	0.887	1.270	23.400	72.0	59.0	409.32
3	2.210	2.220	2.300	2.380	0.929	1.291	2.120	0.130	0.901	1.295	18.600	72.0	59.0	409.32
4	3.690	3.710	3.150	3.250	0.928	1.290	2.900	0.195	0.903	1.280	15.275	72.0	59.0	409.32
5	6.130	6.150	4.400	4.530	0.930	1.288	4.030	0.300	0.901	1.271	12.575	72.0	59.0	409.32
6	10.550	10.580	6.330	6.500	0.931	1.300	5.680	0.470	0.906	1.282	10.572	72.0	59.0	409.32
THE FOLLOWING DATA ARE TAKEN WITH 2.0201 INCH ORIFICE														
7	0.810	0.810	5.800	5.970	0.932	1.315	5.220	0.420	0.908	1.291	11.092	72.0	59.0	409.32
8	1.330	1.330	8.210	8.420	0.934	1.327	7.300	0.646	0.911	1.296	9.330	72.0	59.0	409.32
9	2.210	2.220	12.060	12.300	0.934	1.325	10.670	1.001	0.914	1.287	7.772	72.0	59.0	409.32
10	3.720	3.730	18.050	18.350	0.934	1.345	15.930	1.610	0.918	1.300	6.290	72.0	59.0	409.32
11	6.170	6.150	27.000	27.300	0.934	1.327	23.780	2.470	0.919	1.272	5.148	72.0	59.0	409.32
12	10.110	10.130	40.400	40.850	0.929	1.350	35.220	3.780	0.926	1.294	4.262	72.0	59.0	409.32

SINGLE-BLOW TRANSIENT TEST DATA

PRESSURE DROP RESULTS

CORE NO. 501 AIRES. PLATE-FIN DATA TAKEN ON MARCH 28, 1968 DATA TAKEN BY KLOPFER

HYDRAULIC DIA = 0.002118 FT POROSITY = 0.7441 FRONTAL AREA = 10.533 SQIN KC = 0.19
FLOW LENGTH = 2.570 INCH ALPHA = 1405.1 SQFT/CFT FREE-FLOW AREA = 7.838 SQIN KE = 0.06

RUN	W LB/HR	G LB/HR-SQFT	CORE DP IN.WC	P1 PSI	T1 DEG.F	F	NR
1	91.0	1672.	1.140	14.78	72.51	0.3248	80.1
2	115.9	2129.	1.530	14.78	72.47	0.2688	101.9
3	151.0	2774.	2.120	14.78	73.09	0.2188	132.7
4	194.3	3570.	2.900	14.77	73.18	0.1803	170.7
5	249.1	4577.	4.030	14.77	73.09	0.1521	219.0
6	324.4	5961.	5.680	14.76	73.32	0.1259	285.1
7	239.7	4404.	5.220	14.77	73.41	0.2125	210.6
8	309.5	5613.	7.300	14.76	73.54	0.1822	268.4
9	391.0	7184.	10.670	14.74	73.68	0.1617	343.4
10	502.0	9224.	15.930	14.72	73.86	0.1451	440.8
11	636.9	11701.	23.780	14.69	73.90	0.1328	559.2
12	797.1	14645.	35.220	14.64	74.22	0.1231	699.6

SINGLE-BLOW TRANSIENT TEST DATA

HEAT TRANSFER RESULTS

CORE NO. 501 AIRES. PLATE-FIN DATA TAKEN ON MARCH 28, 1968 DATA TAKEN BY KLOPFER

HYDRAULIC DIA = 0.002118 FT POROSITY = 0.7441 FRONTAL AREA = 10.533 SQIN KC = 0.19
FLOW LENGTH = 2.570 INCH ALPHA = 1405.1 SQFT/CFT FREE-FLOW AREA = 7.838 SQIN KE = 0.06
CORE MASS = 1.9560 LBM CORE SP HT = 0.112 BTU/LB-F COND AREA = 2.280 SQIN
CORE COND = 8.30 BTU/HR-FT-F

RUN	W LB/HR	G LB/HR-SQFT	TBA DEG.F	DTAU SEC	LAMBDA	MAX SLOPE	NTU	NST	J	NR
1	91.0	1672.	80.85	28.800	0.0279	1.246	28.26	0.06988	0.05562	79.2
2	115.5	2122.	81.05	23.400	0.0220	1.208	23.00	0.05687	0.04527	100.5
3	150.0	2756.	81.93	18.600	0.0169	1.170	19.61	0.04848	0.03859	130.3
4	193.1	3547.	81.64	15.275	0.0132	1.107	16.26	0.04019	0.03200	167.8
5	247.5	4547.	81.39	12.575	0.0103	1.049	13.90	0.03438	0.02737	215.2
6	322.2	5919.	81.75	10.572	0.0079	0.959	11.09	0.02742	0.02183	280.0
7	237.8	4369.	82.00	11.092	0.0107	1.238	21.08	0.05212	0.04149	206.6
8	303.0	5567.	82.17	9.330	0.0084	1.155	17.28	0.04273	0.03401	263.2
9	388.2	7133.	82.04	7.772	0.0065	1.082	14.57	0.03602	0.02867	337.2
10	498.0	9150.	82.42	6.290	0.0051	-1.042	13.25	0.03277	0.02609	432.4
11	631.1	11594.	81.82	5.148	0.0040	1.005	12.13	0.03000	0.02388	548.3
12	790.3	14520.	82.47	4.262	0.0032	0.970	11.16	0.02761	0.02198	686.1

Table VI (cont'd) Experimental and Reduced Laboratory Data for Core 501MOD

SINGLE-BLOW TRANSIENT TEST DATA

CORE NO. 501MOD NEW GEOM.PROP DATA TAKEN ON MARCH 6,1968 DATA TAKEN BY KLOPFER

THE FOLLOWING ARE INPUT TEST DATA

RUN	DPOC	DPOH	P1OC	P1OH	T1OC	T1OH	DPS	P1S	T1SC	T1SH	DTAU	TDB	TWB	PAMB
THE FOLLOWING DATA ARE TAKEN WITH 1.3015 INCH ORIFICE														
1	0.790	0.800	0.820	0.850	0.840	1.188	0.770	0.060	0.841	1.241	9.112	68.5	53.0	408.68
2	1.340	1.350	1.140	1.180	0.845	1.194	1.040	0.088	0.849	1.230	7.425	68.5	53.0	408.68
3	2.190	2.200	1.550	1.600	0.854	1.190	1.390	0.130	0.851	1.228	6.275	68.5	53.0	408.68
4	3.700	3.720	2.160	2.230	0.851	1.205	1.900	0.200	0.860	1.239	5.210	68.5	53.0	408.68
5	6.150	6.200	2.990	3.080	0.851	1.210	2.570	0.305	0.860	1.240	4.452	68.5	53.0	408.68
6	10.100	10.120	4.020	4.140	0.856	1.213	3.480	0.460	0.862	1.241	3.815	68.5	53.0	408.68
THE FOLLOWING DATA ARE TAKEN WITH 2.2010 INCH ORIFICE														
7	0.800	0.810	3.770	3.880	0.847	1.198	3.250	0.420	0.860	1.241	3.970	68.5	53.0	408.68
8	1.320	1.330	5.280	5.400	0.849	1.215	4.430	0.650	0.863	1.250	3.385	68.5	53.0	408.68
9	2.210	2.220	7.550	7.730	0.848	1.202	6.200	1.020	0.865	1.229	2.875	68.5	53.0	408.68
10	3.680	3.680	10.850	11.080	0.853	1.228	8.700	1.620	0.855	1.240	2.430	68.5	53.0	408.68
11	6.120	6.160	14.000	16.300	0.850	1.226	12.650	2.540	0.850	1.244	2.018	68.5	53.0	408.68
12	10.190	10.210	23.600	24.000	0.847	1.220	18.350	3.940	0.864	1.269	1.658	68.5	53.0	408.68
13	19.500	19.600	39.500	40.000	0.840	1.202	30.180	6.950	0.861	1.184	1.300	68.5	53.0	408.68

SINGLE-BLOW TRANSIENT TEST DATA

PRESSURE DROP RESULTS

CORE NO. 501MOD NEW GEOM.PROP DATA TAKEN ON MARCH 6,1968 DATA TAKEN BY KLOPFER

HYDRAULIC DIA = 0.001885 FT POROSITY = 0.8965 FRONTAL AREA = 11.139 SQIN KC = 0.08
FLOW LENGTH = 2.562 INCH ALPHA = 1902.1 SQFT/CFT FREE-FLOW AREA = 9.986 SQIN KE = 0.02

RUN	W LB/HR	G LB/HR-SQFT	CORE DP IN.WC	P1 PSI	T1 DEG.F	F	NR
1	91.3	1317.	0.770	14.76	70.40	0.3179	56.2
2	118.5	1709.	1.040	14.75	70.76	0.2546	73.0
3	150.9	2176.	1.390	14.75	70.85	0.2096	92.9
4	195.5	2818.	1.900	14.75	71.26	0.1705	120.3
5	250.9	3617.	2.570	14.75	71.26	0.1398	154.4
6	319.6	4608.	3.480	14.74	71.35	0.1164	196.7
7	308.0	4442.	3.250	14.74	71.26	0.1171	189.6
8	393.6	5676.	4.430	14.73	71.39	0.0975	242.2
9	506.2	7299.	6.200	14.72	71.48	0.0821	311.4
10	648.0	9345.	8.700	14.70	71.03	0.0700	398.9
11	826.9	11923.	12.650	14.67	70.81	0.0620	509.2
12	1050.8	15152.	18.350	14.62	71.43	0.0550	646.5
13	1407.5	20296.	30.180	14.51	71.30	0.0491	866.2

SINGLE-BLOW TRANSIENT TEST DATA

HEAT TRANSFER RESULTS

CORE NO. 501MOD NEW GEOM.PROP DATA TAKEN ON MARCH 6,1968 DATA TAKEN BY KLOPFER

HYDRAULIC DIA = 0.001885 FT POROSITY = 0.8965 FRONTAL AREA = 11.139 SQIN KC = 0.08
FLOW LENGTH = 2.562 INCH ALPHA = 1902.1 SQFT/CFT FREE-FLOW AREA = 9.986 SQIN KE = 0.02
CORE MASS = 0.8345 LBM CORE SP HT = 0.112 BTU/LB-F COND AREA = 0.721 SQIN
CORE COND = 8.30 BTU/HR-FT-F

RUN	W LB/HR	G LB/HR-SQFT	TBA DEG.F	DTAU SEC	LAMBDA	MAX SLOPE	NTU	NST	J	NR
1	90.9	1311.	79.37	9.112	0.0089	1.687	46.77	0.10324	0.08218	55.4
2	117.8	1699.	79.30	7.425	0.0069	1.597	37.63	0.08307	0.06612	71.8
3	150.0	2164.	79.30	6.275	0.0054	1.484	30.15	0.06655	0.05298	91.4
4	194.3	2801.	79.75	5.210	0.0042	1.381	24.86	0.05487	0.04368	118.2
5	249.5	3597.	79.78	4.452	0.0032	1.258	19.90	0.04392	0.03496	151.8
6	317.3	4576.	79.84	3.815	0.0025	1.154	16.32	0.03604	0.02869	193.1
7	306.7	4423.	79.80	3.970	0.0026	1.148	16.13	0.03561	0.02835	186.7
8	391.3	5643.	80.07	3.385	0.0021	1.055	13.35	0.02946	0.02345	238.1
9	502.9	7252.	79.64	2.875	0.0016	0.966	11.00	0.02428	0.01933	306.2
10	642.9	9270.	79.66	2.430	0.0013	0.895	9.24	0.02040	0.01624	391.3
11	821.6	11847.	79.64	2.018	0.0010	0.843	8.07	0.01782	0.01418	500.1
12	1042.8	15038.	80.52	1.658	0.0008	0.808	7.34	0.01620	0.01289	634.1
13	1398.2	20162.	78.54	1.300	0.0006	0.769	6.53	0.01442	0.01148	852.3

Table VII Summary of Basic Heat Transfer and Flow Friction Characteristics of Offset Rectangular Plate-Fin Surfaces

The j and f versus N_R Characteristics from Smoothed Curves

N_R	Core 107		Core 501		Core 501MOD		Surface of Fig. 8	
	j	f	j	f	j	f	j	f
3000	0.00764	0.0339	-	-	-	-	0.00764	0.0339
2000	0.00843	0.0369	-	-	-	-	0.00843	0.0369
1500	0.00910	0.0398	-	-	-	-	0.00910	0.0398
1200	0.00974	0.0430	-	-	-	-	0.00974	0.0430
1000	0.0104	0.0461	0.0117	0.073	-	-	0.0104	0.0460
800	0.0114	0.0510	0.0124	0.077	0.0116	0.0505	0.0114	0.0508
600	0.0129	0.0599	0.0139	0.085	0.0130	0.0568	0.0129	0.0576
500	0.0141	0.0672	0.0152	0.093	0.0142	0.0622	0.0142	0.0635
400	0.0158	0.0783	0.0172	0.104	0.0161	0.0700	0.0161	0.0710
300	0.0185	0.0962	0.0205	0.124	0.0197	0.0845	0.0197	0.0850
200	-	0.131	0.0266	0.162	0.0272	0.113	0.0272	0.113
150	-	-	0.0327	0.198	0.0347	0.142	0.0347	0.142
100	-	-	0.0445	0.270	0.0490	0.196	0.0490	0.196
80	-	-	0.053	0.325	0.0595	0.237	0.0595	0.237
60	-	-	0.067	0.407	0.077	0.301	0.077	0.301
50	-	-	-	-	0.091	0.352	0.091	0.352

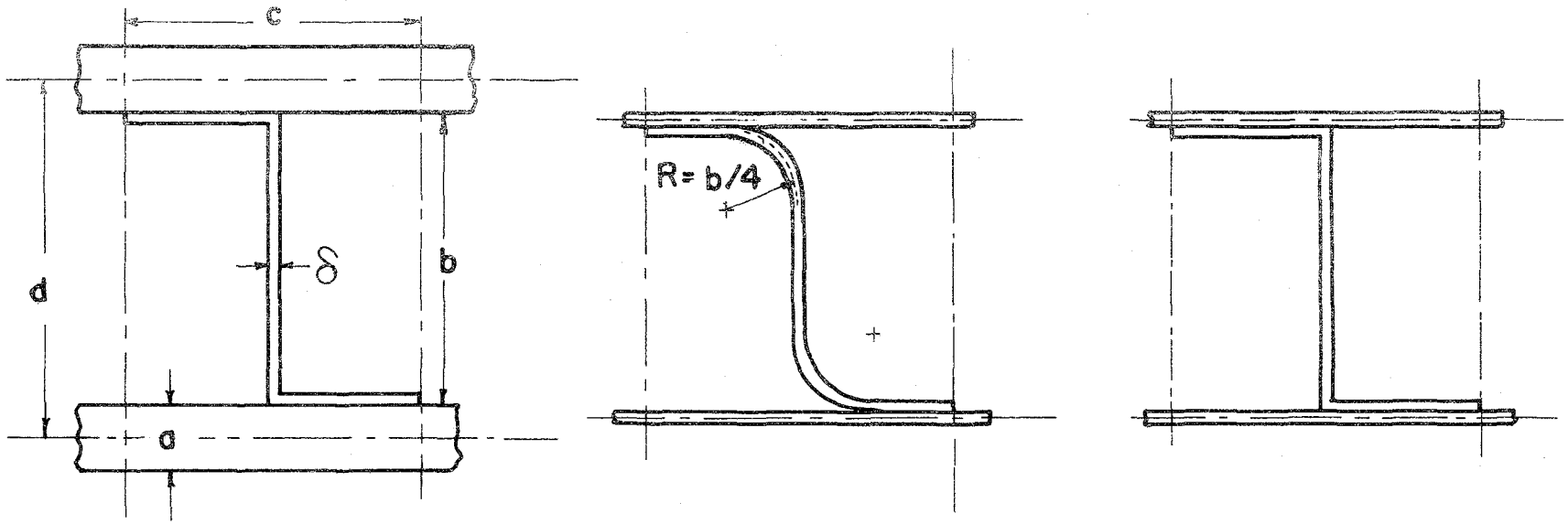

(a) Ideal rectangular model for brazed Core 501

(b) Revised model for unbrazed Core 501MOD

(c) Ideal rectangular model for Core 501MOD

Fig. 11 The Models Used to Derive Core Geometrical Properties

APPENDIX II

SURFACE GEOMETRY RELATIONSHIP

The "cell" geometry for the ideal rectangular model of the flow passage is delineated in Fig. 11(a,c). The core surface is hypothesized to have such identical passages formed by the repetition of the cell geometry. This ideal rectangular model was originally used for evaluation of the geometrical properties of all three cores. But visual inspection revealed that the unbrazed surface (Core 501MOD) did not have a complete mechanical contact between the fins and plate because the corners of the bends are curved rather than sharp at right angle. Consequently, the model in Fig. 11(b) was proposed for the determination of geometrical properties for the Core 501MOD.

The geometry relationships are given here for the purpose of calculating the hydraulic radius r_h, and area density α ft^2/ft^3 in terms of directly measurable quantities, viz., porosity, p, core dimensions, and the cell dimensions. The geometrical relationships are presented for the matrix type Cores 501 and 501MOD. For the steam-to-air heat transfer test core (Core 107) a similar approach is used, taking into account the steam and air header bar heat transfer area, in addition to what is considered below, and the β and r_h are determined from the core dimensions and cell geometry.

Porosity

The surface porosity is an important input to the geometric equations. Once the porosity p is determined the hydraulic radius and the heat transfer area density α ft^2/ft^3 are related by

$$p = r_h \alpha \qquad (8)$$

The surface porosity p is determined from the measurements of effective core mass, effective core volume (length x width x depth) and the density of the core material. Independently, the porosity p is determined geometrically from the cell geometry to verify dimensions of the cell. The actual porosity p is determined from

$$p \triangleq \frac{\text{void volume}}{\text{total volume}} = \frac{\text{(total-solid) volume}}{\text{total volume}}$$

$$p = 1 - \frac{M/\rho_s}{V} \tag{9}$$

where M = core mass, lbm

ρ_s = density of solid material, lbm/ft^3

V = core volume, ft^3

Only the gross measurements are required to accurately determine the porosity p. The geometrically relationships for evaluating the area density α follows for the two models.

Heat Transfer Area Density for Ideal Rectangular Model

The cell geometry is depicted in Fig. 11(a,c). It is assumed that the total length and width of the fin centers are same as those of the plates; otherwise additional area exposed due to difference in the dimensions can easily be added to the following heat transfer area formula.

Wetted perimeter per cell $$P = 2\ (c + b - 2\delta) \tag{10}$$

Heat transfer area excluding edge effect $$A_1 = P\ L\ n \tag{11}$$

Heat transfer of edges A_2

$$A_2 = n\ [2n_{off}\{\delta(c + b - \delta)\} - 2(n_{off}-1)\ \delta(c/2 + \delta/2)] \tag{12}$$

Heat transfer area of plate edges on front and back face } $A_3 = 2n_{plate}\, a\, W$ (13)

Total heat transfer area $A = A_1 + A_2 + A_3$ (14)

Heat transfer area density $\alpha = \frac{A}{V}$ (15)

where n = no. of cells in a flow cross section, $n = (W/c)\,(n_{plate}-1)$

n_{off} = no. of offset in the flow length, $n_{off} = 50$ for Cores 501 and 501MOD

n_{plate} = no. of plates in the test core

W = width of the test core

Knowing α from Eq. (15) and p from Eq. (9), the hydraulic radius r_h is calculated from Eq. (8).

Heat Transfer Area Density for Revised Rectangular Model

The cell geometry is pictured in Fig. 11b. Here also it is assumed that the total length and width of the fin centers are same as those of the plates. The center line radius at the fin and plate joint is assumed to be $R = b/4$.

Wetted perimeter per cell P

$$P = 2\left[c + \{b - 2\,(R + \delta/2)\}\right] + \frac{\pi}{2}\{(R - \delta/2)+(R + \delta/2)\}] \quad (16)$$

Heat transfer area excluding edge effects } $A_1 = P\, L\, n$ (17)

Heat transfer area of edges A_2

$$A_2 = n\,[2n_{off}\{2\delta\,(c/2 - R - \delta/2)\} + \frac{\pi}{2}\{(R + \frac{\delta}{2})^2 - (R - \frac{\delta}{2})^2\} + \delta\{b - 2\,(R+\delta/2)\} - 2(n_{off} - 1)\,(\text{Blocked area})] \quad (18)$$

where

Blocked area per fin = shaded area in the following sketch

$$= \delta\left(\frac{1}{2}c - 2R\right) + \text{area of the sector with the radius } (R + \delta/2) \text{ and height } \delta$$

$$= \delta\left(\frac{1}{2}c - 2R\right) + \frac{\pi(R + \delta/2)^2\theta}{360} - \frac{(R + \delta/2)^2 \sin\theta}{2} \qquad (19)$$

where $\cos(\theta/2) = \dfrac{(R + \delta/2) - a}{R + \delta/2}$

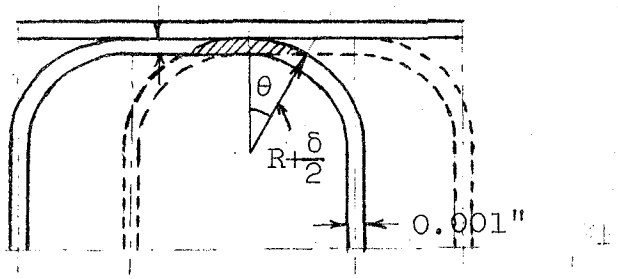

Heat transfer area of the plate edges $A_3 = 2\, n_{plate}\, a\, W$ (20)

Total heat transfer area $A = A_1 + A_2 + A_3$ (21)

Heat transfer area density $\alpha = \dfrac{A}{V}$ (22)

With α from Eq. (22) and p from Eq. (9), the hydraulic radius r_h is found from Eq. (8).

Geometrical Porosity p for the Ideal Rectangular Model

The geometrical porosity p_{geom} for the ideal rectangular model, Fig. 11(a,c) is determined as follows:

cell total area = dc (23)

cell solid area = ac + δ (c + b - δ) (24)

$$p_{geom} = 1 - \frac{ac + \delta(c + b - \delta)}{dc} \qquad (25)$$

Geometrical Porosity p for the Revised Rectangular Model

The geometrical porosity p_{geom} for the revised rectangular model of Fig. 11b is determined as follows:

$$\text{cell total area} = dc \tag{26}$$

$$\text{cell solid area} = ac + \delta\left[2(c/2 - R - \delta/2) + \left\{b - 2(R + \delta/2)\right\}\right] + \frac{\pi}{2}\left[(R + \frac{\delta}{2})^2 - (R - \frac{\delta}{2})^2\right]$$

$$= ac + \delta(c + b - 4R - 2\delta + \pi R) \tag{27}$$

$$p_{geom} = 1 - \frac{ac + \delta(c + b - 0.8584R - 2\delta)}{dc} \tag{28}$$

APPENDIX III

COMPARISON OF STEAM-TO-AIR STEADY STATE AND SINGLE BLOW TRANSIENT HEAT TRANSFER TEST TECHNIQUES

1. Steady State Steam-to-Air Heat Transfer Test Technique

In steam-to-air steady-state test method, the test core is a cross-flow heat exchanger. The steam condenses steadily on one side of the exchanger, and ambient temperature air flows on the other side. The transfer of heat from condensing steam to the air takes place through the wall and fins by conduction and convection from the fluid swept surfaces. The pressure drop on steam side is usually very small, and thus the steam is assumed to condense at a uniform temperature evaluated at an average pressure. As the convection heat transfer coefficient is very high on steam side [3], the wall temperature approximates the temperature of the condensing steam. Thus the heat transfer to air approximates a constant and uniform wall temperature boundary condition (T) .

2. Single Blow Transient Heat Transfer Test Technique

In the single blow transient test method, the test core is a one-fluid-side exchanger with heat transfer only from one fluid to the wall or vice versa. The test core is heated uniformly to a steady state about 20 deg F above the ambient temperature. It is then subjected to a step change in the flowing fluid (air) temperature. The fluid temperature downstream of the matrix is recorded. The heat transfer characteristics is determined from the maximum slope of the downstream fluid temperature-time history, the upstream fluid temperature, the fluid flow rate and the physical properties of the fluid. Actually, in the experiments, two cooling curves and two

heating curves of the downstream fluid temperature are recorded; and the average of the maximum slope from the four traces is employed to determine the convection coefficient, using the one dimensional analysis results provided by Schumann [2,5]. An essential idealization of this analysis is that the convection coefficient is treated as uniform and constant. The result of forcing the experimental results into this model is a mean effective convection coefficient.

In comparing the experimental results for h to theoretical solutions which involve either the idealization of constant and uniform wall temperature (T) or the idealization of constant wall heat transfer flux (H), the question arises as to which set of boundary conditions most closely approximates the test conditions.

As just explained, the experimental heat transfer coefficient h is determined from the maximum slope of the downstream fluid temperature-time history. The temperature of a small slug of fluid passing through the core and reached at downstream of the core is influenced by the wall temperature distribution over which the slug passes. The wall temperature distribution is in turn dependent on the previous history of fluid flow over it. Thus the downstream fluid temperature and the rate of its cooling or heating up to the point of maximum slope depends upon the wall temperature distribution from the time $\tau^* = 0$ to τ^*_{ms} and the space $x = 0$ to L. As a result, the experimentally determined h is ensemble average over space $x = 0$ to L and time $\tau^* = 0$ to τ^*_{ms}.

It was hypothesized by Klopfer and Young [8,12] that as the N_{tu} and hence h is determined from the maximum slope of the downstream fluid temperature-time

history, the h was dependent on the fluid and wall temperature distribution in the core at time $\tau^* = \tau^*_{ms}$. To approximately determine the wall boundary condition for the heat transfer, the non-dimensional fluid and wall temperatures from [2] were plotted in Fig. 12 at time $\tau^* = \tau^*_{ms}$ for several N_{tu} magnitudes. It was concluded from these figures (Fig. 12) that the constant surface temperature (T) , is not close to the reality over N_{tu} range 3 to 30. At low N_{tu} ($\lesssim 5$), however, the constant wall heat flux (H) , corresponding to approximately constant wall to fluid temperature difference appears to be approximated over a significant portion of the flow length. Consequently, the laminar flow theory heat transfer solutions for (H) boundary condition were used to compare with the experimental data in [8,12], even though there appears to be a condition of increasing heat flux (increasing temperature differences) with flow length as the N_{tu} increases beyond 5.

A review of thirteen long cylindrical passage type matrices tested at Stanford [3,7,8,12,13] revealed that the experimental heat transfer data were lower by 10 to 30 percent in all test cores when compared with (H) solutions. The excellent agreement of the test results of Core 501MOD with Core 107 at low N_{tu} (corresponding to high Reynolds number) in Fig. 6 indicates that the convection behavior (h or j) approaches the (T) boundary condition behavior as observed in the steam-to-air heat transfer testing of Core 107. Consequently, it was considered advisable to reexamine the approximate wall boundary condition for the single blow transient heat transfer testing method. This is done in Fig. 13 where the wall temperature t^*_s and the temperature

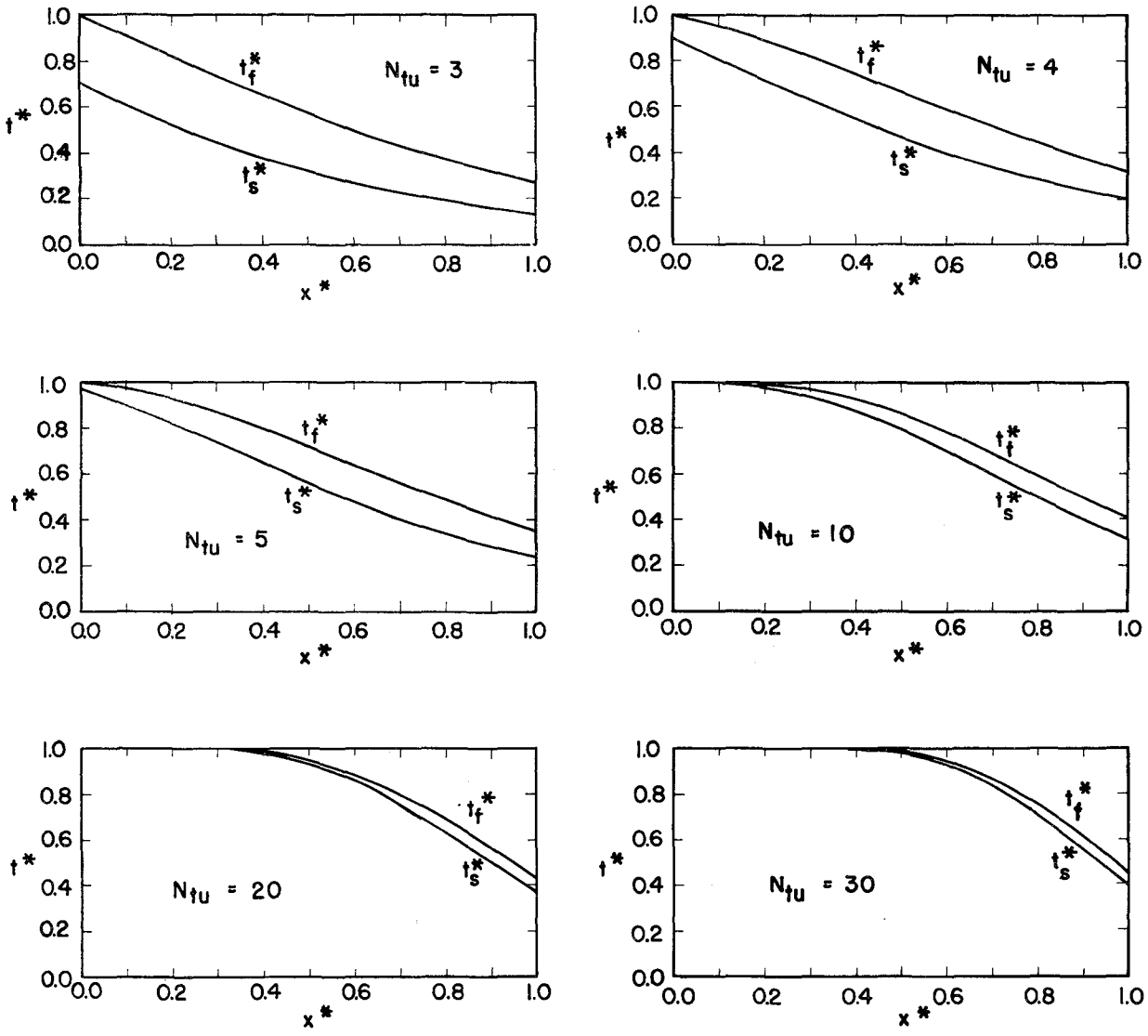

Fig. 12 Normalized Wall and Fluid Temperature Profiles at the Time of Maximum Temperature Change During the Core Heating Cycle of Single Blow Testing

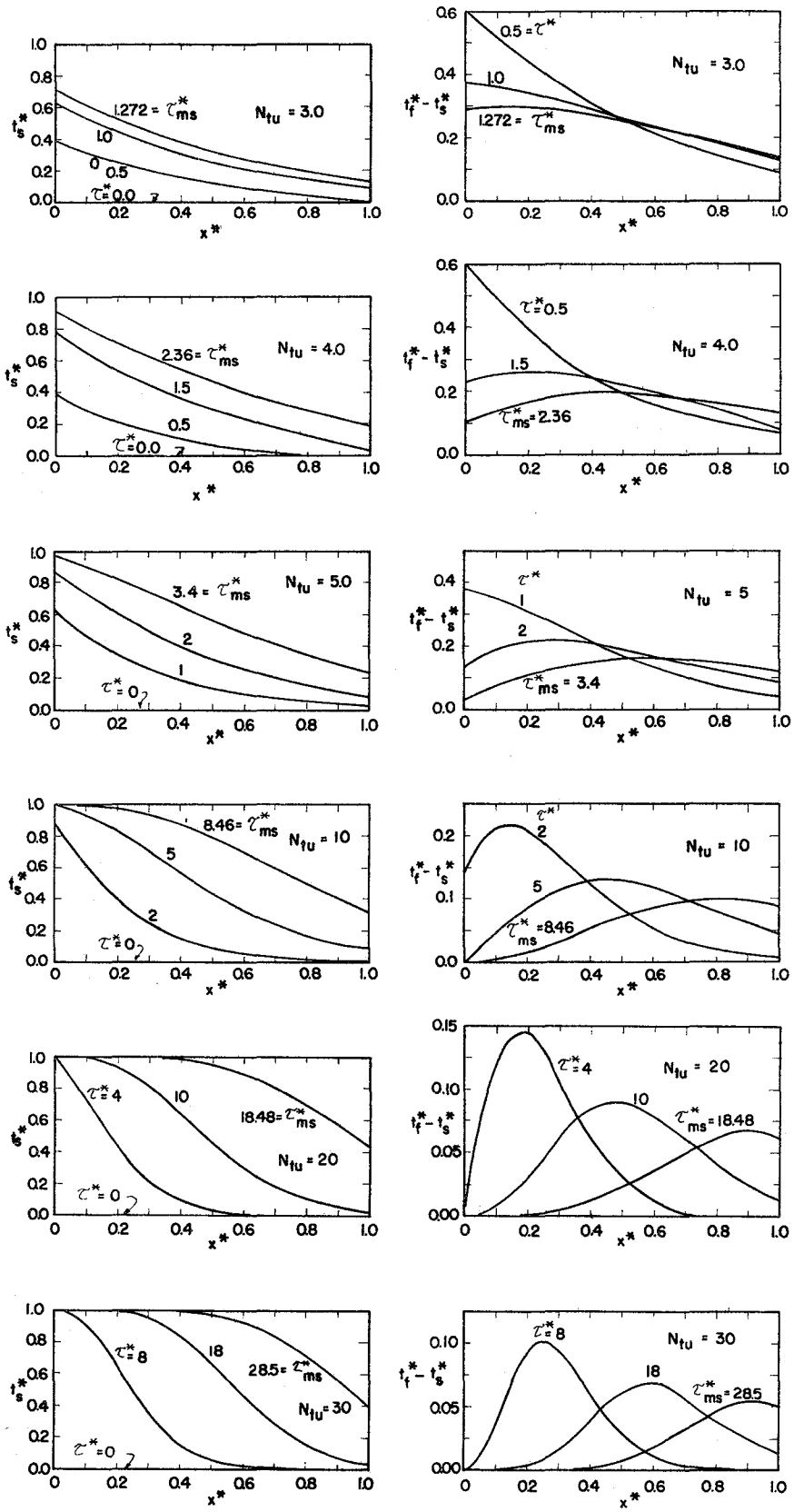

Fig. 13 Normalized Wall Temperature and Fluid to Wall Temperature Difference as Functions of N_{tu} and τ^* for the Core Heating Cycle of Single Blow Testing

difference $(t_f^* - t_s^*)$ are plotted as functions of the axial position x^* and the dimensionless time τ^* for the N_{tu} range of 3 to 30.

For $N_{tu} \leq 2$, the maximum slope for the downstream fluid temperature-time history occurs at time $\tau^* = 0$ [2]. Hence, for $N_{tu} \leq 2$, the constant and uniform wall temperature boundary condition, Ⓣ , for the heat transfer, is an exact representation. From Fig. 13, over most of the time τ^* (from $\tau^* = 0$ to $\tau^* = \tau_{ms}^*$), the wall temperature may be reasonably approximated as constant for N_{tu} between 2 and 3. Thus the Ⓣ boundary condition is the appropriate for the single blow technique with the maximum slope data reduction method for $N_{tu} \leq 3$.

However, the single blow test technique is normally restricted to $N_{tu} \geq 3$ as the uncertainty associated with the maximum slope data reduction method is very high [5]. Thus from the above discussion, at the test core N_{tu} around 3 (the trailing edge of the N_{tu} range of the single blow method), the heat transfer data would be expected to correspond to Ⓣ boundary condition.

In contrast, reviewing Figs. 12 and 13, it appears that the Ⓗ boundary condition seems to be the more appropriate over most of the time up to τ_{ms}^* for N_{tu} of 4 and 5. This implies that there would be a drop of about 20 percent (the difference between $N_{Nu,H}$ and $N_{Nu,T}$) in the heat transfer results for the test core N_{tu} from about 5 to 3. However, examinations of test results of matrices tested at Stanford do not reveal this trend. The heat transfer characteristics $jN_R = N_{Nu} N_{Pr}^{-1/3}$ is found to be essentially constant for the tested matrices confirming that the N_{Nu} is constant, as anticipated by the theory for laminar flow in

long cylindrical passages for either Ⓗ or Ⓣ conditions but not for a "mixture" of the two.

From Fig. 13 at high N_{tu} (>20), examining the temperature difference $(t_f^* - t_s^*)$, it appears that for a constant value of h, the heat flux first increases and then decreases exponentially over the length of the core. According to Hall et al. [14], the fully developed laminar flow heat transfer coefficient h is higher for the exponentially increasing heat flux compared to a constant heat flux; while for exponentially decreasing heat flux, the h is lower. It seems, at high N_{tu}, as a result of these compensating influences, that the overall effect is to approach the value of h corresponding to constant heat flux boundary conditions Ⓗ .

To summarize, it appears qualitatively, on theoretical grounds, that the h at low N_{tu} approaches Ⓣ boundary condition; at high N_{tu}, the h approaches Ⓗ boundary condition, and at intermediate value of N_{tu}, it will be in between. However, this result would show up as a j-N_R characteristic on log log coordinates having a slope less than -1 for fully developed laminar flow surfaces, but this has not been observed [3,13]. At this point, it should be mentioned that passage-to-passage nonuniformities may also be used to rationalize the observed lower j-N_R characteristics of the 13 test cores that were reviewed.

To resolve the open question as to whether or not the Ⓗ or Ⓣ boundary conditions are most appropriate for the transient technique, it is recommended that at least two different well defined heat transfer surfaces, be carefully tested to compare the results with the theory. Such a test matrix could be made up out of circular tubes with $D \leq 0.05$ inch, as an example, and one or more such matrices should be tested over a wide range of N_R and N_{tu}.

A.F. INSTIT. OF TECH. LIB.
BLDG. 640 AREA B
WRIGHT-PATTERSON AFB
OHIO 45433

AFOSR
ATTN: SREM
WASHINGTON, D. C. 20330

ARL (ARIL)
BLDG. 450
W-PAFB, OHIO 45433

DIRECTOR
U.S. ARMY ENGINEERING
RESEARCH AND DEVELOPMENT
LABORATORIES
ATTN: HEAD, NUCLEAR POWER
BRANCH
FORT BELVOIR, VIRGINIA 22060

U.S. ARMY MOBILITY EQUIPMENT (2)
RESEARCH AND DEVELOPMENT CENTER
ATTN: TECHNICAL DOCUMENTS CENTER
BLDG 315, VAULT
FORT BELVOIR, VIRGINIA 22060

(5) U.S. ATOMIC ENERGY COMMISSION
DIVISION OF REACTOR DEVELOPMENT
ATTN: CHIEF, REACTOR COMPONENT
DEVELOPMENT BRANCH
WASHINGTON, D. C. 20545

U.S. COAST GUARD HEADQUARTERS
ATTN: W.S. VAUGHN, CDR.,USCG
TESTING AND DEVELOPMENT DIV.
1300 E STREET
WASHINGTON, D. C. 20002

(20) DEFENSE DOCUMENTATION CENTER
CAMERON STATION
ALEXANDRIA, VIRGINIA,22314

PROF. OF ENGINEERING
U.S. MILITARY ACADEMY
WEST POINT, N.Y. 10996

OFFICE OF THE ADMINISTRATOR
NASA HEADQUARTERS,
1520 H STREET N.W.
WASHINGTON D.C. 20001

NASA
AMES RESEARCH CENTER
ATTN: LIBRARY 202-3
MOFFETT FIELD, CALIF. 94035

NASA
LANGLEY RESEARCH CENTER
ATTN: LIBRARY
LANGLEY STATION
HAMPTON, VIRGINIA, 23365

(2) NASA
ATTN: LIBRARY
LEWIS RESEARCH CENTER
2100 BROOKPARK ROAD
CLEVELAND, OHIO 44135

NAVAL AIR SYSTEMS COMMAND
ATTN: AER-AE-651
DEPARTMENT OF THE NAVY
WASHINGTON, D. C. 20360

(2) NAVAL AIR SYSTEMS COMMAND
ATTN: AIR 536B2
DEPARTMENT OF THE NAVY
WASHINGTON, D.C. 20360

(2) NAVAL AIR SYSTEMS COMMAND
ATTN: PP-22
DEPARTMENT OF THE NAVY
WASHINGTON, D. C. 20360

U.S. NAVAL POSTGRAD. SCH.
ATTN: LIBRARY
MONTEREY, CALIFORNIA 93940

U.S. NAVAL POSTGRAD. SCH.
ATTN: PROF. PAUL PUCCI
MONTEREY, CALIFORNIA 93940

CHIEF OF NAVAL RESEARCH
ATTN: CODE 438
DEPT. OF THE NAVY
WASHINGTON, D. C. 20360

(2) CHIEF OF NAVAL RESEARCH
ATTN: CODE 473
DEPARTMENT OF THE NAVY
WASHINGTON, D.C. 20360

(6) DIRECTOR
NAVAL RESEARCH LABORATORY
ATTN: CODE 2027
WASHINGTON, D.C. 20360

DIRECTOR
NAVAL RESEARCH LABORATORY
ATTN: LIBR., CODE 2029 (ONRL)
WASHINGTON, D.C. 20390

NAVAL SHIP ENGINEERING CENTER
ATTN: DIR. OF RESEARCH
DEPARTMENT OF THE NAVY
WASHINGTON, D. C. 20360

CHARLES L. MILLER (6146)
NAVAL SHIP ENGRG. CENTER
CENTER BUILDING
PRINCE GEORGES CENTER
HYATTSVILLE, MARYLAND 20782

HEAD, COMBINED POWER & GAS TURBINE BRANCH
NAVAL SHIP ENGINEERING CENTER
PHILADELPHIA DIVISION
NAVAL BASE
PHILADELPHIA, PA. 19112

(2)NAVAL SHIP ENGRG. CENTER
ATTN: CODE 312
DEPARTMENT OF THE NAVY
WASHINGTON, D. C. 20360

(2) NAVAL SHIP ENGINEERING CENTER
ATTN: CODE 430
DEPARTMENT OF THE NAVY
WASHINGTON, D. C. 20360

NAVAL SHIP ENGINEERING CENTER
ATTN: CODE 513
DEPARTMENT OF THE NAVY
WASHINGTON, D. C. 20360

NAVAL SHIP ENGRG. CENTER
ATTN: CODE 551
DEPARTMENT OF THE NAVY
WASHINGTON, D. C. 20360

NAVAL SHIP ENGINEERING CENTER
CENTER BUILDING - CODE 6147
PRINCE GEORGES CENTER
HYATTSVILLE, MD. 20782

NAVAL SHIP RES. & DEV. CTR
AERODYNAMICS LIBRARY (CODE L46)
WASHINGTON, D.C. 20007

NAVAL SHIP SYSTEMS COMMAND
NAVSHIPS 08 - ROOM 1301
DEPARTMENT OF THE NAVY
ATTN: J. E. INTRABARTOLO
WASHINGTON, D.C. 20360

COMMANDER, NAVAL SHIP SYST. COM.
TECHNICAL LIBRARY
CODE 2052, RM. 1532 MAIN NAVY BLDG
18TH & CONSTITUTION AVE., NW
WASHINGTON, D.C. 20360

COMMANDING OFFICER
OFFICER OF NAVAL RESEARCH
BRANCH OFFICE
1030 E. GREEN STREET
PASADENA, CALIFORNIA 91101

OFFICE OF NAVAL RESEARCH
FLUID DYNAMICS PROGRAM
CODE 438
WASHINGTON, D.C. 20360

INST. OF TECH. LIB.
MCLI-LIB, BLDG. 125, AREA B
OHIO 45433
WRIGHT-PATTERSON AFB

THE AIR PREHEATER CO.
ATTN: ENGRG. LIBRARY
WELLSVILLE, N.Y., 14895

THE UNIVERSITY OF ALBERTA
UNIVERSITY LIBRARY
PERIODICALS DEPARTMENT
EDMONTON 7, CANADA

AMER. SOC. OF MECH. ENGRS.
UNITED ENGINEERING CENTER
345 EAST 47TH STREET
NEW YORK, NEW YORK 10017

ARGONNE NATIONAL LAB
REPORT SECTION 203CE125
9700 SO. CASS AVENUE
ARGONNE, ILLINOIS 60439

ARO, INCORPORATED
AEDC LIBRARY
ATTN: TECH. FILES
ARNOLD AIR FORCE STN.
TENNESSEE 37389

ATOMICS INTERNATIONAL
ATTN: LIBRARY
P.O. BOX 390
CANOGA PARK, CALIF. 91305

AVCO EVERETT RES. LAB.
ATTN: TECH. LIBRARY
2385 REVERE BEACH PARKWAY
EVERETT, MASSACHUSETTS 02149

BROOKHAVEN NAT. LAB.
ATTN: RES. LIBRARY
TECH. INFO. DIVISION
UPTON, LONG ISLAND, N.Y. 11973

SCIENCES-ENGINEERING LIBRARY
UNIVERSITY OF CALIFORNIA
SANTA BARBARA, CALIFORNIA 93106

CALIF. INST. OF TECH.
MECH. ENGRG. DEPT.
1201 E. CALIFORNIA ST.
PASADENA, CALIFORNIA 91109
LOGAN LEWIS LIBRARY
CARRIER RES. & DEV. CO.
CARRIER PARKWAY
SYRACUSE, NEW YORK 13201

DYNATECH CORP.
17 TUDOR STREET
CAMBRIDGE, MASS. 02138

FERROTHERM COMPANY
FIN TUBE DIV.
14301 SOUTH INDUSTRIAL AVE.
CLEVELAND, OHIO 44137

LIBRARY
GARRETT CORP. AIRESEARCH MFG. DIV.
2525 WEST 190TH STREET
TORRANCE, CALIF. 90509

LIBRARY
GULF GENERAL ATOMIC INC.
P.O. BOX 608
SAN DIEGO, CALIF. 92112

GENERAL ELECTRIC CO.
P & D CENTER
P.O. BOX 43-BLDG. 5-2
SCHENECTADY, N.Y. 12301

FAIRCHILD HILLER
REPUBLIC AVIATION DIV.
ENGINEERING LIBRARY
FARMINGDALE, L.I., N.Y. 11735

MAE DEPT
ILLINOIS INST. OF TECH.
3110 S. STATE STREET
CHICAGO, ILL. 60616

DEPUTY LIBRARIAN, CENTRAL LIBRARY
INDIAN INSTITUTE OF TECHNOLOGY KANPUR
I.I.T. POST OFFICE
KANPUR-16
INDIA

LEAR SIEGLER, INC.
ENGINEERING LIBRARY
P.O. BOX 6719
CLEVELAND, OHIO 44101

MODINE MANUFACTURING CO.
ATTN: LIBRARIAN
1500 DEKOVEN AVENUE
RACINE, WISCONSIN, 53401

W. S. ROBERTS ENGINEERING CO., INC.
1800 N. MERIDAN STREET
INDIANAPOLIS, INDIANA 46202

LIBRARY
SHELL DEVELOPMENT CO.
1400-53RD STREET
EMERYVILLE, CALIF. 94608

RESEARCH REPORTS COLLECTION (3)
ENGINEERING LIBRARY
STANFORD UNIVERSITY
STANFORD, CALIF. 94305

STEWART-WARNER CORP.
ATTN: LIBRARY
1514-DROVER STREET
INDIANAPOLIS, INDIANA 46221

SVERDRUP & PARCEL AND ASSOC., INC.
800 NORTH 12TH BOULEVARD
ATTN: LIBRARY
ST. LOUIS, MO. 63101

SYLVANIA ELEC. PROD INC.
SES-WD, ELECTRONIC DEF. LABS.
TECH REPTS LIBRARY, BLDG. 2
P.O. BOX 205
MT. VIEW, CALIF. 94040

UNIFIED SCIENCE ASSOC., INC.
2925 EAST FOOTHILL BLVD.
PASADENA, CALIF. 91107

ORGDP LIBRARY
UNION CARBIDE CORP. NUCLEAR DIV.
P.O. BOX P
OAK RIDGE, TENNESSEE 37830

UNITED AIRCRAFT CORP.
ATTND CHIEF, LIB. SYSTEM
400 MAIN STREET
EAST HARTFORD, CONN. 06108

ENGRG. SOC. LIBRARY
UNITED ENGRG. TRUSTEES, INC.
345 E. 47TH STREET
NEW YORK, NEW YORK 10017

VITRO CORPORATION OF AMERICA
VITRO LABORATORIES DIVISION
14000 GEORGIA AVENUE
SILVER SPRING, MARYLAND
ATTN: LIBRARIAN

VOUGHT AERONAUTIC DIVISION
LTV AEROSPACE CORPORATION
P.O. BOX 5907
DALLAS, TEXAS 75222
LIBRARY (2-51131)

ENGINEERING LIBRARY
UNIVERSITY OF WASHINGTON
SEATTLE, WASHINGTON 98105

DR. ROBERT C. ALLEN, SR.
644 NORTH 68TH STREET
WAUWATOSA, WISCONSIN 53213

MR. DAVID ARONSON
ADVANCE PRODUCTS DIVISION
WORTHINGTON CORPORATION
BOX 211
LIVINGSTON, NEW JERSEY 07039

MR. A. H. BELL
CHIEF GAS TURBINE ENGRG.
DETROIT DIESEL ENGINE DIVISION
GENERAL MOTORS CORPORATION
13400 WEST OUTER DRIVE
DETROIT, MICHIGAN 48228

YOUNG RADIATOR COMPANY
ATTN: MR. H. E. BRINEN,
V.PRES. EXEC. ENGR.
709 S. MARQUETTE STREET
RACINE, WISCONSIN 53404

MR. DALE H. BROWN
GENERAL ELECTRIC CO.
RESEARCH & DEVELOPMENT CENTER
SCHENECTADY, NEW YORK 12301

PROF. H. BUCHBERG
DEPT. OF ENERGY & KINETICS (5531 BH)
UNIVERSITY OF CALIFORNIA
LOS ANGELES, CALIF. 90024

AMER. SOC. OF HEAT/REFRTG.
AIR-COND. ENGINEERS, INC.
ATTN: J. H. CANSDALE
DIR. P.R.
UNITED ENGRG. CENTER
345 E. 47TH STREET
NEW YORK, NEW YORK 10017

PROF. JOHN C. CHATO
DEPT. OF MECH. AND IND. ENGRG.
UNIV. OF ILLINOIS
URBANA, ILLINOIS 61801

DR. SIMON K. CHEN
V.P. & GEN. MGR. LARGE ENGINES
COLT INDUSTRIES INC.
701 LAWTON AVENUE
BELOIT, WISCONSIN 53511

PURDUE UNIVERSITY
ATTN: PROF. D.S.CLARK
SCHOOL OF MECH. ENGRG.
LAFAYETTE, INDIANA 47905

UNIVERSITY OF MICHIGAN
ATTN: J.A. CLARK
228 W. ENGRG. BLDG.
ANN ARBOR, MICHIGAN 48100

DR. D.L.COCHRAN
M & B ASSOCIATES
P.O. BOX 196
SAN RAMON, CALIFORNIA 94583

PROF. ALBERTO COIMBRA
COPPE-UFRJ
C.P. 1191 - ZC-00
RIO DE JANEIRO - GB
BRASIL

W. A. COMPTON
ASSISTANT DIRECTOR OF RES.
SOLAR
2200 PACIFIC HIGHWAY
SAN DIEGO, CALIF. 92112

PROF. F. A. COSTELLO
DEPT. OF MECHANICAL AND
AEROSPACE ENGINEERING
UNIVERSITY OF DELAWARE
NEWARK, DELAWARE 19711

AEROJET-GENERAL NUCLEONICS
ATTN: SARITA COTTER
3300 CROW CANYON RD.
SAN RAMON, CALIF. 94583

MR. LARRY CUNNINGHAM
CUMMINS ENGINE COMPANY
1000 5TH STREET
COLUMBUS, INDIANA 47201

BATTELLE MEMORIAL INSTITUTE
COLUMBUS LABORATORIES
505 KING AVENUE
COLUMBUS, OHIO 43201
ATTN: JOHN E. DAVIS,
PROJECTS ADMINISTRATOR

MR. R. S. DEGROOTE
SENIOR DESIGN ENGINEER
UNITED AIRCRAFT PRODUCTS, INC.
BOX 1035
DAYTON, OHIO 45401

CORNELL AERONAUTICAL LAB., INC
4455 GENESEE STREET
BUFFALO, NEW YORK 14221
ATTN: J.P. DESMOND, HEAD
LIBRARIAN

CORNELL UNIVERSITY
DEPT. OF THERMAL ENGRG.
UPSON HALL
ATTN: PROF. D. DROPKIN
ITHACA, NEW YORK 14850

MR. E. A. DRURY
3634 BEN STREET
SAN DIEGO, CALIF. 92111

UNIVERSITY OF MINNESOTA
MECH. ENGRG. DEPT.
ATTN: E. R. G. ECKERT
MINNEAPOLIS, MINNESOTA 55455

DR. CHAS C. ECKLES
DIR. OF RES. & DEVELOP.
HARRISON RADIATOR DIVISION
GENERAL MOTORS CORP.
LOCKPORT, NEW YORK 14094

MR. THOMAS L. ECKRICH
41 SUNSET ROAD
BAY SHORE, NEW YORK 11706

WOLVERINE TUBE DIVISION
ATTN: MR. J. EDDENS
17200 SOUTHFIELD ROAD
ALLEN PARK, MICHIGAN 48101

SEND TO:
(1) MR. A. J. EDE
NATIONAL ENGRG. LAB
EAST KILBRIDE
GLASGOW, SCOTLAND

MR. LAMONT ELTINGE
VICE PRES., RESEARCH
CUMMINS ENGINE CO., INC.
COLUMBUS, INDIANA 47201

M. W. KELLOGG CO.
ATTN: MR. G.P. ESCHENBRENN
710 THIRD AVENUE
NEW YORK, NEW YORK 10017

WESTINGHOUSE ELECT. CORP.
ATTN: MR. F. K. FISCHER,
MGR. DEV. ENGRG.
LESTER BRANCH P.O.
PHILADELPHIA, PA. 19113

MR. K. A. GARDNER
LIQUID METAL ENGINEERING CENTER
P.O. BOX 1449
CANOGA PARK, CA. 91304

MR. D. P. GHERE, DIRECTOR
ENGINEERING DESIGN & DEVELOPMENT
RESEARCH & DEVELOPMENT CENTER
ALLIS-CHALMERS
P.O. BOX 512
MILWAUKEE, WISCONSIN 53201

NORTHERN RES. & ENGRG. CORP.
ATTN: MR. K. GINWALA, EXEC. V.P.
219 VASSAR STREET
CAMBRIDGE, MASS. 02139

GENERAL MOTORS CORP.
ATTN: MR. J.W. GODFREY
HARRISON RADIATOR DIV.
LOCKPORT, NEW YORK 14094

MR. STANLEY S. GROSSEL
HOFFMANN-LA ROCHE, INC.
CHEMICAL ENGINEERING DEPARTMENT
340 KINGSLAND ROAD
NUTLEY, NEW JERSEY 07110

MR. ROBERT A. HARMON
DIRECTOR, PROGRAM DEVELOPMENT
MECHANICAL TECHNOLOGY INCORPORATED
968 ALBANY SHAKER ROAD
LATHAM, NEW YORK 12110

DR. A. P. HATTON
MECHANICAL ENGINEERING DEPT.
MANCHESTER COLLEGE OF TECH.
MANCHESTER, ENGLAND

MR. CHRIS HAZELOOP
SENIOR PROJECT ENGINEER
ADVANCED ENGINEERING
PEREFX CORPORATION
7121 DORCHESTER LANE
GREENDALE, WISCONSIN 53129

RICHARD HEROLD, PRES.
SULZER BROS., LTD.
19 RECTOR STREET
NEW YORK, N.Y. 10006

GENERAL ELECTRIC CO.
ATTN: MISS J. HEWITT
MAIN LIBRARY - BLDG. 2
SCHENECTADY, NEW YORK 12305

EDWARD HINES, DIRECTOR
ENGRG. RES. DEPT.
THE DETROIT EDISON CO.
2000 SECOND AVE.
DETROIT, MICHIGAN 48226

AIRESEARCH MFG. COMPANY
ATTN: NELSON W. HOPF, LIBR.
DEPT. 93-32M
402 SOUTH 36TH STREET
PHOENIX, ARIZONA 85034

PROFESSOR C. P. HOWARD
MECHANICAL ENGINEERING DEPT.
THE CATHOLIC UNIVERSITY
WASHINGTON, D. C. 20017

ATOMIC POWER DEV.
ASSOCIATES, INC.
ATTN: DR. WAYNE H. JENS
DETROIT, MICHIGAN 48226

MR. AL JOHNSON
AEROSPACE CORP.
BLDG A2, MAIL STOP 2037
2300 E. EL SEGUNDO BLVD.
EL SEGUNDO, CA. 90045

MR. A. L. JOHNSON
ELECTRO THERMO ASSOCIATES
504 STRAND
MANHATTAN BEACH, CALIF. 90266

THE KRAISSL CO., INC.
ATTN: F. KRAISSL, JR.
229 WILLIAMS AVENUE
HACKENSACK, NEW JERSEY 07604

MR. GEORGE J. KIDD JR.
UNION CARBIDE CORPORATION
P.O. BOX P, BLDG. K1401
OAK RIDGE, TENN. 37830

DR. G. F. KOHLMAYER
SCIENTIFIC ANALYSIS
ENGINEERING BUILDING 264
PRATT & WHITNEY AIRCRAFT
EAST HARTFORD, CONN. 06108

MR. S. KOPP, MANAGER
NUCLEAR PRODUCTS DEPT.
STRUTHERS WELLS CORP.
WARREN, PA. 16365

UNIVERSITY OF COLORADO
ATTN: PROF. FRANK KREITH
DEPT. OF MECH. ENGRG.
BOULDER, COLORADO 80302

PROF. A.D.K. LAIRD, DIR.
UNIVERSITY OF CALIFORNIA
SEA WATER CONVERSION LAB.
1301 SOUTH 46TH STREET
RICHMOND, CALIF. 94804

PROF. SHANKAR LAL
DEPT. OF MECH. ENGRG.
UNIVERSITY OF ROORKEE
ROORKEE, U.P., INDIA

NEW YORK UNIVERSITY
ATTN: PROF. FRED LANDIS
DEPT. OF MECH. ENGRG.
UNIVERSITY HEIGHTS
NEW YORK, NEW YORK 10019

PROF. MILTON B. LARSON
DEPT. OF MECHANICAL AND
INDUSTRIAL ENGINEERING
OREGON STATE UNIVERSITY
CORVALLIS, OREGON 97331

MR. E. J. LEFEVRE
DEPT. OF MECH. ENGRG.
QUEEN MARY COLLEGE
MILE END ROAD
LONDON E.1, ENGLAND

MR. SYLVESTER LOMBARDO
MGR. TURBINE COMPONENTS
WRIGHT AERONAUTICAL DIVISION
CURTISS-WRIGHT CORPORATION
WOODRIDGE, NEW JERSEY 07440

OAK RIDGE NATIONAL LAB.
ATTN: MR. R. N. LYON
9204-1; Y-12
P.O. BOX Y
OAK RIDGE, TENNESSEE 37831

DR. J. J. MCMULLEN
17 BATTERY PLACE
NEW YORK, NEW YORK 10004

MR. RAYMOND MACHACEK
NET AIR POLLUTION CONT. ADMIN.
DIV. OF MOTOR VEHICLES
RESEARCH AND DEVELOPMENT 3
300 S. THAYER
ANN ARBOR, MICHIGAN 48105

CALIF. RESEARCH CORP.
ATTN: J.H.MCPHERSON
576 STANDARD AVENUE
RICHMOND, CALIFORNIA 94804

MR. DIVEN MEREDITH
PRESSURE COOL CO.
46-025 ARABIA
PO DRAWER Y
INDIO, CALIF. 92201

LOCKHEED AIRCRAFT CO.
ATTN: B.L. MESSINGER,
ENGRG. N. 7225
TECHNICAL LIBRARY
BURBANK, CALIFORNIA 91500

PROFESSOR DARRYL E. METZGER
DEPT. OF MECH. ENGRG.
ARIZONA STATE UNIVERSITY
TEMPE, ARIZONA 85281

PROF. HAROLD S. MICKLEY
DIR. OF CTR. FOR ADV. ENGRG. STUDY
M.I.T. ROOM 9-215
77 MASS. AVENUE
CAMBRIDGE, MASS. 02139

ARGONNE NATIONAL LABS
ATTN: DR. DAVID MILLER, 208
REACTOR PHYSICS DIVISION
9700 SOUTH CASS AVENUE
ARGONNE, ILLINOIS 60439

PROF. J. W. MITCHELL
DEPT. OF MECH. ENGRG.
UNIVERSITY OF WISCONSIN
MADISON, WISCONSIN 53706

PROF. R. W. STUART MITCHELL
LABORATORIUM VOOR VERBRAN-
DINGSMOTOREN EN GASTURBINES
DER TECHNISCHE HOGESCHOOL
MEKELWEG 2
DELFT, HOLLAND

CATERPILLAR TRACTOR CO.
ATTN: MISS CAROL E. MULVANEY
RESEARCH LIBRARIAN
TECHNICAL CENTER
PEORIA, ILL. 61602

VIRGINIA POLYTECHNIC INST.
ATTN: CAROL M. NEWMAN
LIBRARY
BLACKSBURG, VIRGINIA 24060

R. H. NORRIS
RES & DEV. CENTER,
GENERAL ELECTRIC CO.
6TH FLOOR, BLDG. 37
P. O. BOX 43
SCHENECTADY, NEW YORK 12301

H. V. NUTT
NAVAL SHIP RESEARCH AND
DEVELOPMENT LAB.
ANNAPOLIS, MARYLAND 21402

UNIVERSITY OF WISCONSIN
ATTN: PROF. E. OBERT
1513 UNIVERSITY AVE.
MADISON, WISCONSIN 54306

UNIVERSITY OF CALIF.
ATTN: PROF. A. OPPENHEIM
COLLEGE OF ENGRG.
BERKELEY, CALIFORNIA 94720

ARGONNE NATIONAL LABS
ATTN: MR. M. PATRICK
9700 SOUTH CASS AVENUE
ARGONNE, ILLINOIS, 60440

PROF. J. T. PEARSON
SCHOOL OF MECH. ENGRG.
PURDUE UNIVERSITY
LAFAYETTE, INDIANA 46207

UNIVERSITY OF SANTA CLARA
ATTN: PROF. R. K. PEELEY
SANTA CLARA, CALIF. 95053

R. C. PERPALL
5433 WHITEFOX DRIVE
PALOS VERDES ESTATES,
CALIF. 90274

C.F. BRAUN AND CO.
ATTN: MR. EARL PHILLIPS
MURRAY HILL, NEW JERSEY 07971

H. PHILLIPS, ASSOC. DIR. RES.
FOSTER WHEELER CORP.
110 SO. ORANGE
LIVINGSTON, NEW JERSEY 07039

MRS. L. B. PHILLIPS, SUPTDT.
TECH. INFO. SEC.
SCIENTIFIC RESEARCH STAFF
FORD MOTOR COMPANY
P.O. BOX 2053
DEARBORNE, MICHIGAN 48121

BROWN FINTUBE CO.
P.O. BOX 3499
TULSA, OKLAHOMA 74101
ATTN: MR. JERRY J. PIKE

(2) SOLAR AIRCRAFT CO.
ATTN: MR. P. A. PITT
VICE PRES. ENGRG/RES.
SAN DIEGO, CALIF. 92112

MR. DICK QUAN
CHIEF PROJECT ENGINEER
ORINDA DIV.
HAWKER SIDDELEY OF CANADA LTD.
53 ASHMONT CRESENT
WESTON, ONTARIO, CANADA

MR. GEORGE RENKER
ATTN. DIV. LIBRARY
AVCO LYCOMING DIVISION
550 SOUTH MAIN STREET
STRATFORD, CONN. 06497

D. W. RETZINGER
3737 N. WISCONSIN STREET
RACINE, WIS. 53402

MASS INST. OF TECH.
ATTN: W. M. ROHSENOW
MECH. ENGINEERING RM 1-212
CAMBRIDGE, MASS. 02139

(2) THE TRANE COMPANY
ATTN: MR. H. C. ROOKS
LA CROSSE, WISCONSIN 54601

DR. C. G. A. ROSEN
261 HAMILTON AVENUE
PALO ALTO, CALIFORNIA 94301

K. C. ROSENBERT, SUPERVISOR
TECH. DOCUMENT CENTER
ATTN: MS E-110
HUGHES AIRCRAFT COMPANY
FLORENCE AND TEALE STREETS
CULVER CITY, CALIF. 90230

PROFESSOR M. A. SAAD
DEPARTMENT OF MECH. ENGRG.
UNIVERSITY OF SANTA CLARA
SANTA CLARA, CALIF. 95050

MR. L. P. SAUNDERS
P. O. BOX L
CARMEL, CALIF. 93921

MR. WOLFGANG SCHAECHTER
THIOKOL CHEMICAL CORP.
ASTRO-MET DIVISION
P.O.BOX 1497
OGDEN, UTAH 84402

DR. F. A. SCHRAUB
APED, MAIL CODE 583
175 CURTNER AVENUE
GENERAL ELECTRIC CO.
SAN JOSE, CALIF. 95125

PROF. F. L. SCHWARTZ
DEPT. OF MECH. ENGRG.
UNIVERSITY OF FLORIDA
GAINESVILLE, FLA. 32601

PERFEX CORPORATION
ATTN: MR. W. W. SCHWID
500 WEST OKLAHOMA AVE.
MILWAUKEE, WISCONSIN 53207

UNIVERSITY OF CALIFORNIA
ATTN: PROF.R.A.SEBAN,M.E.
COLLEGE OF ENGRG.
BERKELEY, CALIFORNIA 94720

DR. J. RODGER SHIELDS
DIRECTOR OF ENGRG.
ELLIOTT COMPANY
JEANNETTE, PA. 15644

MR. EDWARD SIMONS
BOX 299
MILL VALLEY, CALIF. 94943

MR. R. SIMS
HEAT EXCHANGER PROJECT
LEYLAND GAS TURBINES LIMITED
METEOR WORKS
SOLIHULL, WARWICKSHIRE
ENGLAND

UNIVERSITY OF NEW MEXICO
ATTN: PROF. B.S.SKOGLUND
DEPT. OF MECH. ENGRG.
ALBUQUERQUE, NEW MEXICO 87106

FORRESTAL CAMPUS LIBRARY
PRINCETON UNIVERSITY
P.O. BOX 710
ATTN: M. H. SMITH, LIB.
PRINCETON, N.J. 08540

UNIVERSITY OF ILLINOIS
ATTN: PROF. S. L. SOO
MECHANICAL ENGINEERING DEPT.
URBANA, ILLINOIS 61801

BROWN BOVERI CORP.
ATTN: E. H. STAUFFER
STAFF ASSISTANT
1460 LIVINGSTON AVE.
NORTH BRUNSWICK, N.J. 08902

THE CATHOLIC UNIV. OF AM.
ATTN: PROF. J. STEFFENS
DEPT. OF MECH. ENGRG.
WASHINGTON, D. C. 20017

NORTH AMERICAN ROCKWELL CORPORATION
ATTN: M. A. SULKIN
INT'L AIRPORT, LOS ANGELES
CALIFORNIA 90009

W. A. SUTHERLAND
GENERAL ELECTRIC CO.
175 CURTNER AVE MC 584
SAN JOSE, CALIF. 95125

MR. IVAN M. SWATMAN, CHIEF ENGINEER
TURBINE OPERATIONS ENGINEERING OFFICE
FORD MOTOR COMPANY, P.O. BOX 2053
DEARBORN, MICHIGAN 48121

MASS. INST. OF TECH.
ATTN: E. S. TAYLOR
GAS TURBINE LAB.
CAMBRIDGE, MASS. 02139

MR. E. TIEFENBACHER
DAIMLER-BENZ AKTIENGESELLSCHAFT
7 STUTTGART - UNTERTORKHEIM
GERMANY

GENERAL ELECTRIC COMPANY
2151 SO. 1ST STREET
ATTN: F.E. TIPPETS
ATOMIC POWER EQUIP. DIV.
SAN JOSE, CALIFORNIA 95112

MR. A. TOPOUZIAN
FORD MOTOR CO.
ENGINEERING STAFF
AMERICAN ROAD
DEARBORNE, MICHIGAN 48121

TUFTS UNIVERSITY
ATTN: DR. TREFETHEN
MECH. ENGRG. DEPT.
MEDFORD, MASS. 02155

GENERAL MOTORS CORP.
ATTN: MR. W. A. TURUNEN,
ENGRG. DEV. DEPT.
RESEARCH LABORATORIES
12 MILE MOUND ROADS
WARREN MICHIGAN 48090

AUBURN UNIVERSITY
ATTN: PROF.D. VESTAL,
CHAIRMAN
DEPT. OF MECH. ENGRG.
AUBURN, ALABAMA 36830

MR. DAVID J. S. WARDALE
CORNING GLASS WORKS
TECH. PROD. DIVISION
CERCOR HEAT EXCHANGERS
CORNING, NEW YORK 14830

WESTINGHOUSE ELECT. CORP.
ATTN: DR. STEWART WAY
RESEARCH LABORATORY
BEULAH ROAD
PITTSBURGH, PA. 15235

ATTN: MR. R. L. WEBB
THE TRANE COMPANY
LA CROSSE, WISCONSIN 54601

THE BABCOCK & WILCOX CO.
RES. & DEV. CENTER
ATTN: C.P. WELCH
P.O. BOX 835
ALLIANCE, OHIO 44601

MR. JOHN W. WELLS
PROJECT ENGINEER, FB2G5
PRATT & WHITNEY AIRCRAFT
EAST HARTFORD, CONN. 06108

MRS. LINDA KESSLER, LIBRARIAN
ENGINEERING DIVISION
THE TRANE COMPANY
LA CROSSE, WISCONSIN 54601

MR. STANLEY WONG
1128 WEST 126TH STREET
LOS ANGELES, CAL. 90044

MR. CLIFFORD C. WRIGHT
4638 BROWNDEER LANE
PALOS VERDES PENINSULA
CALIFORNIA 90274

DR. ROGER M. WRIGHT
AIRESEARCH MFG. CO.
6235 MONITA STREET
LONG BEACH, CALIF. 90814

MR. DICK ZEEK
DETROIT DIESEL ENGINE DIVISION
GENERAL MOTORS CORPORATION
13400 WEST OUTER DRIVE
DETROIT, MICHIGAN 48228

PROF. RICHARD W. ZEREN
DEPARTMENT OF MECHANICAL ENGINEERING
MICHIGAN STATE UNIVERSITY
EAST LANSING, MICHIGAN 48823

Security Classification

DOCUMENT CONTROL DATA - R & D

(Security classification of title, body of abstract and indexing annotation must be entered when the overall report is classified)

1. ORIGINATING ACTIVITY (Corporate author)	2a. REPORT SECURITY CLASSIFICATION
Stanford University Mechanical Engineering Stanford, California 94305	Unclassified
	2b. GROUP

3. REPORT TITLE

THE INFLUENCE OF BRAZING ON VERY COMPACT HEAT EXCHANGER SURFACES

4. DESCRIPTIVE NOTES *(Type of report and inclusive dates)*

5. AUTHOR(S) *(First name, middle initial, last name)*

Ramesh K. Shah, A. L. London

6. REPORT DATE	7a. TOTAL NO. OF PAGES	7b. NO. OF REFS
November 1, 1970	44	14

8a. CONTRACT OR GRANT NO.	9a. ORIGINATOR'S REPORT NUMBER(S)
Nonr 225(91) b. PROJECT NO.	TR No. 73
c.	9b. OTHER REPORT NO(S) *(Any other numbers that may be assigned this report)*
d.	

10. DISTRIBUTION STATEMENT

The distribution of this document is unlimited.

11. SUPPLEMENTARY NOTES	12. SPONSORING MILITARY ACTIVITY
	Office of Naval Research NR 090-342 Washington, D.C. 20360

13. ABSTRACT

Three geometrically similar offset rectangular plate-fin surfaces with area densities in the range from 900 to 2000 ft^2/ft^3 were tested to establish the heat transfer, $j\text{-}N_R$, and flow friction, $f\text{-}N_R$, characteristics. The Reynolds number range was from 60 to 3000. One surface was unbrazed while the other two, because of a two-to-one difference in plate, fin and offset spacing dimensions, were characterized by different degrees of brazing"roughness".

The test results reveal a relatively small effect of brazing on $j\text{-}N_R$, but a significant influence on $f\text{-}N_R$, with a 35 to 50 percent higher friction for the brazed surface. There is an "area penalty" of 14 percent due to brazing associated with the complete coverage of the interface area at the brazed joints. The magnitude of this penalty depends on the geometry of the surface.

DD FORM 1 NOV 65 1473

Security Classification

14 KEY WORDS	LINK A		LINK B		LINK C	
	ROLE	WT	ROLE	WT	ROLE	WT
Compact heat exchangers, influence of brazing						
Heat exchangers, design data						
Plate-Fin surfaces						